

A CALORIMETRIC STUDY OF THE INTERACTIONS
OF LANTHANIDE PERCHLORATES IN
ACETONITRILE WITH WATER AND
WITH DIMETHYL SULFOXIDE

By

JAMES CALVERT CANNON

Bachelor of Science

Oklahoma State University

Stillwater, Oklahoma

1969

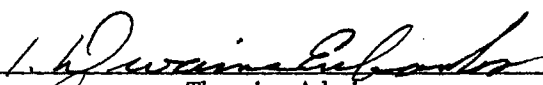
Submitted to the Faculty of the Graduate College
of the Oklahoma State University
in partial fulfillment of the requirements
for the Degree of
DOCTOR OF PHILOSOPHY
December, 1973

Thesis
1973D
C226c
cop. 2

JUN 17 1975

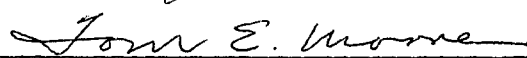
A CALORIMETRIC STUDY OF THE INTERACTIONS
OF LANTHANIDE PERCHLORATES IN
ACETONITRILE WITH WATER AND
WITH DIMETHYL SULFOXIDE

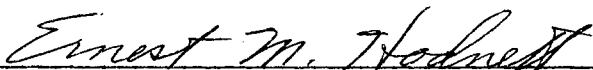
Thesis Approved:

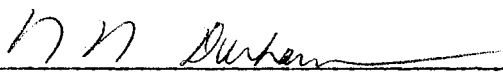


Thesis Adviser









Dean of the Graduate College

911064

PREFACE

I wish to express my deepest gratitude to my research adviser, Dr. I. Dwaine Eubanks for his guidance and encouragement throughout the course of this study. Dr. Thomas E. Moore and Dr. Neil Purdie also provided many helpful suggestions and comments, and Dr. Otis C. Dermer offered valuable assistance in the preparation of the final manuscript.

I am grateful for the financial support made available to me in the form of a summer research fellowship from Phillips Petroleum Company, a National Defense Education Act research fellowship, a National Science Foundation Summer Traineeship, and a teaching assistantship from the Oklahoma State University Department of Chemistry. Additional support from the Oklahoma State University College of Engineering in the form of an appointment as Freshman Chemistry Tutor is also acknowledged.

Dr. Gordon Wallace gave me much practical advice regarding the operation of the calorimeter, and Geoffrey McArthur helped me to organize the filing system for my references.

My parents gave me an appreciation of the value of an education, and the means to obtain it.

Most of all, I must thank my wife, Juanita, who endured the irregular hours and ill-considered outbursts which accompanied the completion of this project. Her, particularly, I owe beyond any possibility of repayment.

TABLE OF CONTENTS

Chapter	Page
I. INTRODUCTION.	1
Historical	1
Changes in Coordination Number.	2
Ligand Field Effects.	4
Changes in Hydration Number	4
Combined Effects.	5
Nonaqueous Systems.	6
Statement of the Problem	7
II. METHOD OF STUDY	10
Successive Complex Formation	10
Calorimetric Studies of Complex Formation.	12
Computational Approach	14
III. EXPERIMENTAL.	19
Materials.	19
Reagents.	19
Rare Earth Oxides.	19
Perchloric Acid.	19
Acetonitrile	19
Karl Fischer Reagent	19
Disodium ethylenediaminetetraacetate (EDTA).	19
Dimethyl sulfoxide	19
Water.	19
Molecular Sieve.	20
Nitrogen	20
Perchlorate Solutions	20
Analysis of Working Solutions	23
Water Content.	23
Metal Concentration.	23
Calorimeters	24
Temperature Measuring Circuitry	24
Electrical Calibration Circuitry.	26
Mechanical System	27
Performance	29
Titration Procedure.	29

TABLE OF CONTENTS (Continued)

Chapter	Page
IV. DATA REDUCTION.	33
Chart Displacements.	33
Calories Per Mole of Salt.	34
Stability Constants and Stepwise Enthalpies.	35
Main Program.	36
Subroutine ACE.	37
Subroutine ACEX.	41
Subroutine CON.	41
Subroutine DXNV.	42
Subroutine FFCT.	43
Error Limits.	43
V. RESULTS AND DISCUSSION.	45
Heats of Mixing of Ligands and Acetonitrile.	45
Metal-Ligand Titrations.	46
Results from Water System.	47
Results from the DMSO System.	53
Discussion of Standard States and Activities.	62
Discussion of Factors Affecting Complex Stability.	65
VI. SUMMARY AND SUGGESTIONS FOR FUTURE WORK	72
A SELECTED BIBLIOGRAPHY	74
APPENDIX A - COMPUTER PROGRAM AND EXPERIMENTAL DATA	77
APPENDIX B - FLOW CHARTS.	88

LIST OF TABLES

Table	Page
I. Comparison of Values Calculated for the Ag-Pyridine System by Direct Search Method with Originally Reported Literature Values.	17
II. Thermodynamic Results for Water System Calculated from Truncated Data Set	50
III. Thermodynamic Results for Water System Calculated from High Order Data Set.	52
IV. Graphically Estimated and Numerically Calculated Limiting Coordination Numbers	57
V. Thermodynamic Results for DMSO System Calculated from Truncated Data Set	60
VI. Thermodynamic Results for DMSO System Calculated from High Order Data Set.	63

LIST OF FIGURES

Figure	Page
1. A Schematic Diagram of Temperature Measurement and Calibration Circuits of Calorimeter.	25
2. Mechanical Parts of Calorimeter (See Text for Explanation of Parts Labelled A-E)	28
3. Recording Potentiometer Trace Resulting from Temperature Change Within Calorimeter, with Baseline Extended to Allow Measurement of Attendant Displacement	31
4. Plot of h_1 as a Function of $1/r_{ion}$ for Water System.	51
5. Plot of $\Delta\bar{H}$ as a Function of C_L for Ho-DMSO Titrations.	54
6. Hypothetical Plots of $\Delta\bar{H}$ as a Function of C_L for the Cases of Complete and of Incomplete Reaction	55
7. Plot of Graphically Estimated Limiting Coordination Number as a Function of $1/r_{ion}$	56
8. Use of Plot of $\Delta\bar{H}$ vs $1/r_{ion}$ to Estimate the Free Ligand Concentration, $[L]$ at Some Value of C_L	58
9. Plot of h_1 as a Function of $1/r_{ion}$ for DMSO System	61

LIST OF SYMBOLS

ΔG	Gibbs free energy
ΔG°	Standard Gibbs free energy
G	Function used in Newton-Raphson calculation
G'	First derivative of function G
K	Equilibrium constant
K_n	Successive (stepwise) formation constant for ML_n
β_n	Overall formation constant for ML_n
$\Delta \bar{H}$	Calories evolved per mole of salt
ΔH°	Standard enthalpy change
ΔH_n	Successive (stepwise) enthalpy change for ML_n
h_n	Overall enthalpy change for ML_n
ΔS	Entropy change
ΔS°	Standard entropy change
ΔS_n	Successive (stepwise) entropy change for ML_n
s_n	Overall entropy change for ML_n
C_M	Total analytical concentration of M
C_L	Total analytical concentration of L
C_P	Heat capacity at constant pressure
$[M]$	Concentration of free M
$[L]$	Concentration of free L
α_n	Fraction of C_M in form of ML_n
α_{nk}	Fraction of CM in form of ML_n at the k^{th} data point

LIST OF SYMBOLS (Continued)

r_{ion}	ionic radius
Q	Calories evolved
V	Sample volume in calorimeter
i	Calibration heater current (subscript is used as index, also)
E	Calibration heater voltage
t	Calibration time
c	Chart displacement
U	Error squared sum
D.F.	Number of degrees of freedom
v	Calculated variable
σ_v	Standard deviation associated with calculated variable v

CHAPTER I

INTRODUCTION

Since World War II, much research has been done on the coordination chemistry of lanthanide ions in solution (1) (2). Much of the practical interest in the area has been due to the need to separate the lanthanides from other elements produced in nuclear reactors. Of late, additional impetus has resulted from the report by Hinckley (3) that the presence of paramagnetic rare earth ions and their complexes in solution causes large shifts in the proton NMR spectra of various organic molecules. An understanding of the factors which affect the stability of rare earth complexes in solution would be useful in both of these areas of applied lanthanide chemistry.

Historical

There have been extensive reviews of the literature pertaining to lanthanide coordination chemistry in the past decade (1) (2). From these reviews, it is clear that most research in the area has involved measurement of the change in free energy, ΔG , associated with the formation of rare earth complexes in aqueous solution and with attempts to explain the observed trends in the stability of the complexes. Experimental efforts have centered on studying the formation of complexes with the anions of aminopolycarboxylic acids.

Correlations have been made between the stability of the complexes and the ionic radii of the trivalent lanthanide ions. If a purely electrostatic model were sufficient to explain the stability trends observed for complexes of a given ligand as one varies the metal ion across the lanthanide series, then one would expect a logarithmic plot of complex stability vs. the reciprocal of the ionic radius to be a straight line (1). In fact, however, the plots of $\log K$, where K is the equilibrium constant, against $1/r_{\text{ion}}$ have proven to be non-linear (2). Changes in coordination number, changes in the solvation of the metal ion, and ligand field effects have all been invoked to explain the observed trends (2).

Changes in Coordination Number

Wheelwright, Spedding, and Schwarzenbach (4) measured the stability constants of the complexes formed between the trivalent rare earth ions and the anion of ethylenediaminetetraacetic acid (EDTA). Two experimental methods were employed: a potentiometric method and a polarographic method. In both, the reactions studied involved competition between copper ions and the rare earth of interest, and all measurements were made in aqueous solution at constant ionic strength. A plot of $\log K$ versus atomic number showed a general increase with a discontinuity in the region of Gd(III). There is no corresponding discontinuity in the ionic radii. A sterically induced change in coordination number was proposed as an explanation. It was suggested that as the ionic radius decreases, the bulky carboxylate groups have increasing difficulty in finding enough room near the ion during coordination. As the lanthanide ionic radius decreases, a point is reached beyond which only three

carboxylate groups can be coordinated. At this point, near the middle of the series, a break in the plot of $\log K$ versus atomic number is observed.

Diethylenetriaminepentaacetic acid (DTPA) has also been used as a ligand by Harder and Chaberek (5). The potentiometric method just described was used. In this case, a plot of $\log K$ versus $1/r_{\text{ion}}$ showed an even more pronounced discontinuity in the middle of the series, in the form of a plateau in stability extending from Sm to Er. A possible change in the coordination number of the metal with increasing atomic number and decreasing ionic radius is again advanced as an explanation.

Moeller and Ferrus (6) measured the enthalpy changes for the formation of N-(2-hydroxyethyl)ethylenediaminetriacetic acid (HEDTA) by potentiometrically following in the equilibrium constant as a function of temperature in water at constant ionic strength, according to the equation

$$-\log K = \frac{\Delta H}{2.303 RT} + \text{constant} \quad (1)$$

The equilibrium constants at 25°C were used to calculate ΔG , and ΔS was then evaluated by the relation

$$\Delta G = \Delta H - T\Delta S \quad (2)$$

They suggest that there is some sort of gradual alteration in the internal degrees of freedom of the ligand as a result of coordination to different metals in the series. Steric hindrance is viewed as the cause of this gradual alteration. The enthalpy data reported are consistent with this explanation in that one expected effect of increasing steric hindrance would be for one of the carboxylate groups to become less firmly attached to the metal ion. Similar studies by Moeller and Thompson (7) on DTPA and by Moeller and Hseu (8) on trans-1,2-diaminocyclohexane-N,N,

N',N'-tetraacetic acid (DCTA) support this conclusion. Hoard and co-workers (9) (10) have determined the crystal structure of hydrated Lanthanide-EDTA complexes by x-ray diffraction. These studies indicate three or four water molecules (depending on the exact environment in the primary coordination sphere of the lanthanide ion) in addition to the EDTA. It would seem appropriate to consider these additional ligands in any explanation of the coordination behavior of lanthanides with EDTA.

Ligand Field Effects

Yatsimirskii and Kostromina (11) have examined the splitting of the 4f energy levels for the rare earth ions in fields of cubic, octahedral, and tetrahedral symmetry. The ligand-field stabilization energies predicted are of the correct magnitude to explain the nonlinearity of the $\log K$ versus $1/r_{\text{ion}}$ plots for the EDTA complexes, assuming that EDTA is hexadentate in the systems and that the symmetry of the complexes is approximately octahedral. It is pointed out that different ligands would have different field strengths, relative to water, and this is invoked to explain the differences in trends observed for different ligands.

Changes in Hydration Number

Edelin De La Praudiere, and Staveley (12) measured the heats of formation for the 1:1 complexes of the lanthanide ions with nitrilotriacetic acid (NTA) by differential calorimetry. A plot of ΔH versus atomic number for this series of complexes reveals a minimum at Sm and a maximum at Er. This shape is explained in terms of a change in hydration number occurring near the middle of the series which is superimposed on the effect of the change in ionic radius. Padova (13) has calculated

the hydration numbers of rare earth ions from partial molal volume data. These calculations, while inconclusive, are consistent with the interpretation of the NTA data.

Combined Effects

Tereshin (14) has surveyed the literature and pointed out that the ligand field effect should manifest itself most clearly in ΔH , and that since ΔG , and hence $\log K$, is affected by ΔS as well as ΔG , one should be very cautious about inferring the existence or nonexistence of a ligand field effect from stability constant data alone. He concluded that the observed trends in rare earth complex stability can best be explained by postulating the existence of a ligand field effect and a change in the number of water molecules which are displaced by a given ligand as one varies the identity of the metal.

Staveley, Markham, and Jones (15) (16) have made calorimetric measurements of the integral heats of solution of the ethyl sulfates and the bromates of the lanthanides. These salts are isomorphous across the lanthanide series, and this property is used in the construction of a thermochemical cycle in which the effects of a possible change in hydration number are believed to be eliminated. This thermochemical cycle is used to estimate the heats of formation of lanthanide complexes in dilute solution starting with the rare-earth as the solid ethyl sulfate or bromate. For the 1:3 diglycolate and dipicolinate complexes, the calculated ΔH 's show a trend which is consistent with the presence of a ligand field effect.

Morss (17) has performed a study similar to the work of Staveley, Markham, and Jones previously described. Heats of solution for the

complex chlorides $\text{Cs}_2\text{NaMCl}_6$, where M is a lanthanide ion, were measured calorimetrically. Lattice energies were calculated and used in a Born-Haber cycle to determine ionization potentials and hydration enthalpies. Morss concludes that the thermodynamic stability trends can be explained in terms of variations in the lattice parameters of the solids, without recourse to a ligand-field effect.

Karraker (18) has reviewed the literature pertaining to the coordination behavior of the lanthanides in the trivalent state. He concludes that while the evidence for coordination effects in solution is generally indirect, there are very strong indications that change in the coordination number of lanthanide ions in solution with decreasing ion size is as definite and as important as in crystals of their salts.

Nonaqueous Systems

Forsberg and Moeller (19) have used titration calorimetry to measure the enthalpy of complexation of lanthanide perchlorates with ethylenediamine in anhydrous acetonitrile. They observed the formation of stable complexes containing one, two, three, and four ethylenediamine molecules. ΔH_1 and ΔH_2 became increasingly exothermic monotonically as the ion size diminished, but ΔH_3 and ΔH_4 exhibited minima at Dy^{+3} and Tb^{+3} respectively. The behavior of ΔH_3 and ΔH_4 was attributed to a change in solvation occurring gradually across the series. Initially, it was postulated, the decrease in ion size makes the solvent and previously attached ligand molecules more tightly bound and consequently the enthalpy change involved in replacing solvent with ethylenediamine becomes less exothermic. Gradually, steric factors begin to make one or more solvent molecules more labile later in the series, and the enthalpy change for

adding ethylenediamine becomes exothermic.

D. O. Johnston and co-workers (20) (21) have measured the electrical conductance for anhydrous lanthanide chlorides in ethanol and for both the chlorides and bromides in methanol. In each of these systems, a maximum is reported in the molar conductance at Gd, as compared to similar studies in water which show a general decrease with decreasing ionic radius. This set of observations is explained by hypothesizing that the solvent complexes with the metal ion more strongly at the middle of the series than at the ends. The ligands involved are ranked in order of decreasing coordination strength as $\text{H}_2\text{O} > \text{MeOH} > \text{EtOH} > \text{NO}_3^- > \text{Cl}^- > \text{Br}^-$ and it is noted that this order generally follows the spectrochemical series for the d-orbital splitting of the transition elements. The chlorides of La and Yb in ethanol have essentially the same temperature coefficient of conductance, and this is supposed to indicate that both La and Yb have about the same effect on the structure of ethanol.

In a somewhat related study, Merbach, Pitteloud, and Jaccard (22) report that the solubilities of lanthanide chlorides in 2-propanol exhibit a maximum at Dy, although no explanation is advanced. In contrast, they report the solubilities in ethanol and methanol increase all the way across the period.

Statement of the Problem

Most of the previous studies of the complexation of the rare earth ions have suffered from several shortcomings. The use of multidentate ligands has introduced the possibility that changes in the coordination number and configuration of the ligand will obscure any possible ligand field effect. Water is a strongly coordinating solvent, which has

limited the choice of ligand to those which form relatively robust complexes. In addition, water is a highly structured solvent, and possible reordering of the ion's solvation sheath upon complexation would add another complicating factor. Many previous workers have measured only the change in free energy, whereas, as Tereshin has pointed out, more detailed interpretation is possible if ΔH and ΔS are also available.

The purpose of this study was to obtain a complete thermodynamic description (ΔG , ΔH , and ΔS) of rare earth complex formation for a system or systems in which the ligand was definitely monodentate and in which interaction of the anion and solvent with the metal would be lessened. To this end, the interaction of selected rare earth perchlorates in acetonitrile with water and with dimethyl sulfoxide (DMSO) was studied by titration calorimetry.

Lanthanide perchlorates were chosen because, although one would expect ion pairing in an organic solvent of moderate dielectric constant, perchlorate is reported to interact with the lanthanide ions less strongly than nitrate (19).

Acetonitrile was chosen as the solvent because it is polar enough to dissolve the perchlorates, but should have much less structure than water or an alcohol because the absence of hydroxyl groups rules out hydrogen bonding between the solvent molecules. In addition, acetonitrile has been the solvent in previous studies (19).

Water was chosen as a ligand because it is a small molecule which forms monodentate complexes. It was hoped that a study of aquo complex formation would shed some light on the possibility that changes in hydration are responsible for the observed trends in the formation of other complexes.

Dimethyl sulfoxide was chosen as another ligand. It should also form monodentate complexes, and since DMSO cannot hydrogen bond like water, possible preferential reordering of the solvent sphere, as reported by Wallace (23) for the aquo complexes of transition metals in 1-butanol, would be avoided.

Titration calorimetry was chosen as the experimental method. It offers a convenient method of determining ΔG , ΔH , and ΔS simultaneously for a reaction (24). It suffers from the limitation that it gives no information about which species are actually present in solution and thus one must test various chemically reasonable models of the system and accept as probably correct the model which best reproduces the experimental data.

CHAPTER II

METHOD OF STUDY

Successive Complex Formation

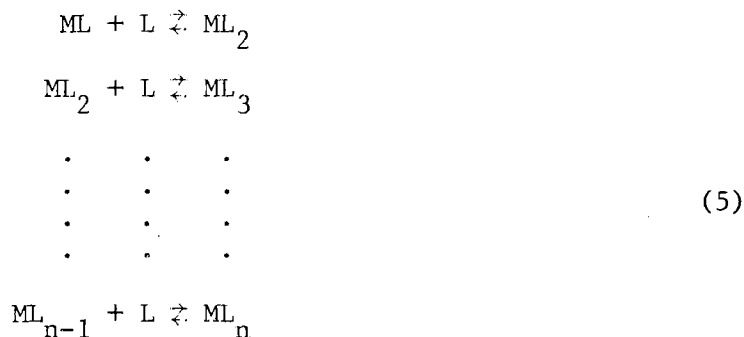
Consider a metal ion, M, which reacts with some ligand, L. We might write the equation for the reaction as



with the equilibrium constant, K, neglecting activity corrections, given by

$$K = [ML] / [M][L] \quad (4)$$

where the bracketed quantities are molar concentrations. (Activity corrections and the rationale for neglecting them are discussed in Chapter V.) The initial product may take part in further reactions as follows:



with stepwise equilibrium constants taking the general form

$$K_n = [ML_n] / [ML_{n-1}][L] \quad (6)$$

Alternatively, we could consider the net reactions:



The overall stability constant for the complex is written as

$$\beta_n = \frac{[ML_n]}{[M][L]^n} \quad (8)$$

These two formulations of stability constant expressions are equivalent, with the relation between them being

$$\beta_n = \prod_{i=1}^n (K_i) \quad (9)$$

Since one set of constants is easily calculated from the other, methods yielding either are discussed without further explanation.

The symbols ΔH_n and ΔS_n represent the stepwise changes in enthalpy and entropy for the formation of the n^{th} complex as presented in Equation 5. The symbols h_n and s_n refer to the overall changes in enthalpy and entropy for formation of the n^{th} complex as represented in Equation 7. The quantities ΔH_n and h_n are related by the expression

$$\Delta H_n = h_n - h_{n-1} \quad (10)$$

and ΔS_n and s_n are related by

$$\Delta S_n = s_n - s_{n-1} \quad (11)$$

As in the case of the stability constants, each set of enthalpies (or entropies) may be calculated from the other.

The total concentration of the metal, its analytical concentration (C_M), is equal to the sum of the concentrations of the metal-containing species

$$C_M = [M] + [ML] + [ML_2] + \dots \quad (12)$$

and in similar manner, the analytical concentration of the ligand is

$$C_L = [L] + [ML] + 2[ML_2] + \dots \quad (13)$$

Equation 8 can be rearranged to obtain

$$[ML_n] = \beta_n [M][L]^n \quad (14)$$

and by substituting expressions of this form into Equations 12 and 13,

one arrives at the results

$$C_M = [M] + \sum_{n=1}^N \beta_n [M] [L]^n \quad (15)$$

and

$$C_L = [L] + \sum_{n=1}^N (n \cdot \beta_n [M] [L]^n) \quad (16)$$

If Equations 15 and 16 can be solved for the free ligand and free metal concentration, Equation 14 can then be used to calculate the concentration of a species of interest. The quantity α_n is defined as the fraction of the total metal concentration which is present in the solution in the form of the n^{th} complex

$$\alpha_n = [ML_n] / C_M \quad (17)$$

Beck (25) points out that Equation 3 represents an oversimplification. The ligand must displace solvent molecules which are attached to the central metal ion in order to form the complex. The process could be more accurately represented



where S is the solvent molecule. Further possible complications might involve rearrangement of the coordination sphere and interactions involving the anion. Such effects are frequently invoked to explain the observed properties of complex species in solution.

Calorimetric Studies of Complex Formation

Calorimetry is a very general method for obtaining information about complex formation (24). As long as the reaction involves a non-zero change in enthalpy (ΔH), either endothermic or exothermic, the temperature change associated with the process can be measured. If the heat capacity of the system (C_p) is known, one can calculate the number of calories absorbed or evolved (Q) by the relation

$$Q = C_p \cdot \Delta T \quad (19)$$

The change in enthalpy is equal to Q for a process occurring at constant pressure (26). If there are no other processes, or if correction can be made for their contribution, calorimetry can be used to determine ΔH for a chemical reaction.

If the reaction under study occurs to an appreciable degree but does not go to completion under the chosen experimental conditions, it is possible to determine the equilibrium constant, K , for the reaction from calorimetry along with ΔH (24). For the simple case of a 1:1 complex, one may write



and

$$Q = \Delta H [ML]V \quad (21)$$

where ΔH is now in calories per mole of ML formed and V is the sample volume in liters. One may combine Equations 12, 13, 14, and 21 to get

$$\frac{\Delta H}{K} = (V \cdot C_M \cdot C_L / Q) (\Delta H)^2 - (C_M \cdot C_L) \Delta H + Q/V \quad (22)$$

The quantities of metal and ligand introduced into the calorimeter are known, and ΔH and K are considered to be constant over the concentration range used. Thus, if Q is measured at two different reagent concentrations, two equations and two unknowns result and both ΔH and K can be calculated from calorimetric data.

The change in Gibbs free energy (ΔG) is related to the equilibrium constant (K) by the equation

$$\Delta G = RT \ln K \quad (23)$$

After solving for ΔG and applying the relation

$$\Delta G = \Delta H - T\Delta S \quad (24)$$

the change in entropy (ΔS) which accompanies the reaction can be calculated.

Computational Approach

As was stated above, for a system in which one complex is formed, the computational problem involves the solution of two equations for two unknowns. In a system with N complexes, there are $2N$ unknowns, and the equations involve terms of higher order than quadratic. These systems cannot be solved exactly, so iterative methods are used. Basically, one guesses solutions to the equations and accepts as correct the set of guesses which best reproduces the original data.

The "best" set of stability constants and ΔH 's is considered to be the one which minimizes the error-squared sum (U) where

$$U = \sum_{k=1}^M (Q_{\text{meas}} - Q_{\text{cal}})_k^2 \quad (25)$$

for M experimental measurements, Q_{meas} , where Q_{cal} is a function of the total concentrations of the reagents and the unknown enthalpies and equilibrium constants. U_{min} is calculated for all models which seem to be chemically reasonable, and the model which gives the lowest U_{min} is taken to be correct.

Izzat and co-workers (27) have discussed four basic approaches to solving the equations which must be solved to obtain stability constants from calorimetric data. They are direct solution of the equations, a grid search, pitmapping, and variable metric minimization (VMM).

Since the relation between the measured heats and the stability constants is nonlinear for cases in which more than one complex is formed, direct solution is not generally feasible for systems with

multiple complexes. A variation sometimes permitting direct solution involves converting the experimentally determined function into one that is linear in the stability constants. Standard linear least square methods are then applied. Bjerrum's (28) Corresponding Solutions treatment is such a method. It has been successfully applied to the formation of aquo complexes of the transition metals (23).

In a grid search, a large number of U's (corresponding to many different combinations of changes in the stability constants) are calculated (27). This method is the most straightforward for dealing with systems which have relative minima in the U-surface. The true minimum can be identified as the lowest one observed over a large range of possible solutions. This method requires a large amount of computer time.

In pitmapping, one assumes a functional form for the U-surface, calculates some trial values of U, and uses them to solve for the minimum of the assumed U-function (29). This method uses less computer time than the grid search, but must have fairly good initial guesses for the constants if it is to converge on a solution.

In VMM, one varies a stability constant in some semi-random manner and accepts or rejects this change according to whether U decreases or increases (30). This method is somewhat slower than pitmapping but converges over a wider range of initial guesses. VMM has been successfully applied to the formation of aquo complexes, but reportedly failed to converge in cases where more than two complexes were considered to be present at the same time (23). As VMM is generally carried out, exploratory moves are made across the U surfaces to gain information about the surface's shape. A pattern move is then made in the direction

indicated by the exploratory moves. This is also called a pattern search.

A similar technique is called a direct search (31). (This method is not to be confused with the previously mentioned "direct solution.") In this case, one makes successive random guesses and keeps any new guesses which lower the value of U . This method, which has been compared to a blind man crawling down a hill on his hands and knees, is somewhat slower than a pattern search, but much simpler to program.

Calculations based on the results of preliminary experiments showed the Corresponding Solutions approach to be unsuitable for the current problem. The first few ligands added to each metal ion form complexes which are sufficiently stable for the free ligand concentrations to be small, relative to C_L . As a result, small errors in the experimental data frequently caused the apparent value of the free ligand concentration to be negative and the computational method failed. It should be possible to apply the Corresponding Solutions approach to a truncated data set in order to calculate the stability constants for the later, weaker successive complexes. A similar truncation process was used in some of the actual calculations. This is discussed in Chapter IV.

Conventional direct solution was impossible, since more than one complex is formed. Grid search methods were ruled out by the amount of computer time required. The VMM pattern search was considered undesirable because of the difficulties reported in obtaining convergence with large models.

Programs were written using both pitmapping and direct search approaches. The Ag-pyridine complexes were used as a test case because calorimetric data were available and because the system involved the

formation of two successive complexes (32). Two complexes are sufficient to provide a nonlinear case but the system is still small enough that the programs can run quickly. This system has previously been used to test computer programs for the calculation of stability constants (27).

The pitmapping program gave the correct ΔH 's when the initial guesses of the constants were the answers from the literature, but if bad guesses were used as a starting point, the program would not converge at all closely on the literature values. It may be that the author's version of the program uses some numerical method which is ill-suited for the particular equations being treated and that some alternative version would work substantially better. This approach was discarded.

The direct search method gave ΔH values and stability constants which fell within the error limits of the results in the literature, even with poor initial guesses. The results are shown in Table I. This method was adopted.

TABLE I
COMPARISON OF VALUES CALCULATED FOR THE Ag-PYRIDINE SYSTEM
BY DIRECT SEARCH METHOD WITH ORIGINALLY
REPORTED LITERATURE VALUES

Quantity Calculated	Value from Reference 32	This Work
β_1	2.00 \pm 0.04	2.07 \pm 0.05
β_2	4.11 \pm 0.04	4.12 \pm 0.04
ΔH_1	4.83 \pm 0.05	4.79 \pm 0.03
ΔH_2	11.34 \pm 0.01	11.33 \pm 0.01

One might note that both the VMM direct search method and the pit-mapping method suffer from an important shortcoming. If the initial guesses are near a relative minimum, the methods may both converge on the relative minimum rather than the absolute minimum. It is possible to partially guard against this by trying several sets of guesses on various sides of the presumed minimum and seeing that all trials give the same answer within reasonable error limits.

The technique used to minimize U is conceptually simple but requires a large number of arithmetic operations. In the direct search program used in this study, initial guesses are made of the stability constants for an assumed model of the system. Using these constants, the Newton-Rapson (33) iterative technique is used to calculate the free metal and free ligand concentrations at each experimental point from C_M and C_L . The free metal and free ligand concentrations and stability constants are used in Equation 14 to calculate the concentrations of each of the species ML_n and these calculated concentrations are used in a linear least square procedure to calculate the enthalpies of formation for the complexes. The error-squared sum (U) is then calculated with these constants. One constant is varied, and the process is repeated to see if the new U is lower than the old. The change in the constant is retained or rejected depending on whether U is lowered. The process is repeated with all constants until eventually a set of values is obtained such that any change in a constant would increase the error-squared sum. The resulting set of constants are the best obtainable for the model under consideration. The details of the logic involved and the way it is implemented on the computer are presented in detail in Chapter IV.

CHAPTER III

EXPERIMENTAL

Materials

Reagents

Rare Earth Oxides. 99.99% pure oxides of the trivalent lanthanides were obtained from American Potash and Chemical Corporation and used without further purification.

Perchloric Acid. Reagent grade 70% perchloric acid was purchased from Allied Chemical Company, and used without further purification.

Acetonitrile. Matheson, Coleman and Bell, Mallinckrodt, Baker, and Fisher Scientific brands of reagent grade were used without purification or were dried by storing over calcium hydride with intermittent shaking for at least two days. The acetonitrile was then distilled before using. Karl Fischer analysis of the dried acetonitrile showed its water concentration to be ~0.001M.

Karl Fischer Reagent. Stabilized solutions from Fisher Scientific were diluted with Baker or Mallinckrodt reagent grade absolute methanol.

Disodium ethylenediaminetetraacetate (EDTA). Baker reagent grade was used without further purification.

Dimethyl sulfoxide. Fisher Scientific reagent grade was dried over molecular sieve for 48 hours and filtered.

Water. Laboratory deionized water was passed through a column of reagent grade Rexyn #300 mixed bed resin (Fisher Scientific Company) and

Molecular Sieve. Linde Molecular Sieve, Type 4A, was activated by heating in a muffle-furnace to 350°C for 24 to 48 hours.

Nitrogen. Linde lamp grade nitrogen was used to purge equipment.

Perchlorate Solutions

Rare earth perchlorates were prepared from the oxides by treating the oxides with slightly less than a 3:1 stoichiometric amount of 1M perchloric acid. This quantity was chosen to insure an excess of the oxide rather than perchlorate. The mixtures were stirred from 4 to 24 hours. This was necessary, since some of the oxides react slowly with the acid at room temperature and insoluble products were sometimes produced when the aqueous solutions were heated. After stirring, the solutions were filtered through a fine-fritted Buchner funnel. The filtered solutions were placed in a desiccator and attached to a vacuum line. The samples were pumped on the vacuum line until most of the bulk water was removed and a tacky solid was left. The solid was then dissolved in acetonitrile.

A number of methods have been reported for obtaining anhydrous non-aqueous solutions of nonvolatile solutes. Three which were tried in this study include placing the non-aqueous salt solution in direct contact with molecular sieve, refluxing the solvent over molecular sieve, and removing the water-acetonitrile azeotrope by fractional distillation. The last method was ultimately adopted for reasons described below.

Placing the salt solution in direct contact with molecular sieve produces very dry solutions. However, previous studies have reported the samples to become contaminated with iron from the sieve (34). Samples of lanthanum perchlorate were analyzed by atomic absorption for

Na, K, Mg, Fe, and Al before and after drying by this method and had picked up nothing but a trace of Na. The lanthanum, however, decreased approximately 30% because metal ion was apparently adsorbed on the sieve. This method was not used for this reason.

In the reflux method, the salt solution is placed in a modified Soxhlet extractor (35). The organic-water mixture is boiled, and the condensed vapors are passed over molecular sieve which traps the water, and the organic solvent is returned to the original solution. When this method was applied to the samples in this study, the solutions developed a brownish color which was attributed to decomposition of the solvent and/or the salt.

In one case, an explosion occurred while using the reflux method. About 15 grams of cerium(III) perchlorate were present in about 500 ml of acetonitrile refluxing in a one-liter vessel. The explosion completely demolished the heating mantle and reflux apparatus and did substantial damage to the laboratory. The severity of the explosion hindered investigation of its cause by destroying most of the evidence, but it had been observed that the solution was taking on the color characteristic of cerium(IV) prior to the blast. Since solutions of lanthanide perchlorates (in addition to cerium) had shown some evidence of decomposition, it was decided to abandon this procedure.

Harris and Moore (36) have used a modification of the reflux method in which 1-butanol solutions of divalent transition metal perchlorates were refluxed over molecular sieve at reduced pressure. This allowed the solution to boil at lower temperatures. It was felt that the use of lower temperatures (approximately 30°C) would lessen the problem of decomposition, but with the rare earth perchlorates, it was not possible

to obtain solutions with a metal-to-water mole ratio of greater than 1:1 even after 15 days of refluxing.

Azeotropic distillation has been used previously to remove some of the bulk water from butanol solutions prior to drying by the reflux method under reduced pressure (23). Pure acetonitrile boils at 82.0°C , and it forms a binary azeotrope with water having a boiling point of 75.6°C and a composition of 83.7% acetonitrile and 16.3% water (37). Thus, it is possible to reduce the water concentration in an acetonitrile solution by fractional distillation.

Acetonitrile solutions of rare earth perchlorates were fractionally distilled, using a silvered vacuum-jacketed distillation column 15 inches long and a variable-reflux-ratio distillation head. The solutions were distilled rapidly at first, using a 1:1 reflux ratio. After the temperature at the head reached about 77°C , the reflux ratio was changed to 10:1 to allow a closer approach to equilibrium conditions.

Initially, the solutions were about 0.05 M in rare earth ions. They were thus concentrated to about 2/3 to 1/2 of their initial volume. The metal concentration and water concentration were then determined. If the metal-to-water ratio was 5:1 or greater, the distillation was terminated. Otherwise, dry acetonitrile was added and the process continued.

At a metal-to-water ratio of about 6:1, the gadolinium perchlorate solution began to show a slight discoloration. Since this occurred even in the absence of molecular sieve, the reflux process does not appear to be responsible for the previously observed decomposition. In no case has any visible decomposition been observed until after the sample has been drying for several days. Prolonged heating may be responsible, or

the salts may become less stable after the last water is removed. In any event, drying was stopped, as a safety measure, when the samples reached a metal-to-water ratio of 5:1. This process took from 48 to 72 hours.

After the stock solutions were prepared and dried by the azeotropic distillation method, they were diluted to the desired working concentrations with dry acetonitrile. The working solutions were stored in glass bottles with serum stoppers in a desiccator and their water content and metal concentration were determined immediately before use.

Analysis of Working Solutions

Water Content. Solutions were analyzed for water by Karl Fischer titration (38). The end-point was detected potentiometrically, using polarized platinum electrodes, and a Beckman Expandomatic II expanded scale pH meter as the null-point detector (39). Karl Fischer reagent was standardized just before use by titration of a 70 mg. sample of distilled water.

Metal Concentration. The concentration of the rare earth was determined by EDTA titration using Arsenazo indicator (40). The sample was diluted with distilled water and sodium hydroxide solution was added until the sample solution was basic to methyl red. Pyridine was added to buffer the system, the indicator was added, and the sample titrated to an orange-pink endpoint. The EDTA was standardized by dissolving an accurately weighed quantity of 99.99% pure samarium(III) oxide in nitric acid and diluting to a known volume with distilled water, then titrating as above.

Calorimeters

The calorimeters used in the study were previously constructed and described by Moore and co-workers (23). Calorimeters of 35 ml and 65 ml capacity were used. They have similar temperature-measuring circuitry and titration heads, and share the same calibration circuit, temperature controller, and chart recorder.

Temperature Measuring Circuitry

A thermistor is the temperature-sensing element in each calorimeter. The thermistor is incorporated into one arm of a Wheatstone bridge (Figure 1). The change in temperature inside the calorimeter changes the resistance of the thermistor, resulting in an imbalance in the bridge circuitry. This imbalance is displayed in analog form on a Sargent model SRG recording potentiometer, which serves as a null-detector.

In the 65 ml calorimeter, a 100-kiloohm Victory Engineering Co. thermistor is used. The resistance R_1 in the bridge is also 100 kiloohms, to allow balancing the bridge. The variable resistors are Borg precision helipots. The bridge is powered by a Trygon Electronics constant voltage source operated at 10.0 volts.

The 35 ml calorimeter uses a 2-kiloohm thermistor, and R_1 is also 2 kiloohm. A decade resistance box serves as the variable resistance. The thermistor has a positive temperature coefficient and is manufactured by Pennsylvania Electronics Technology, Inc. Thermistors with positive temperature coefficients have greater temperature coefficients of resistance than the conventional type ($40\%/^{\circ}\text{C}$ vs $4\%/^{\circ}\text{C}$). However, the manufacturer's specifications indicated that an operating voltage to the

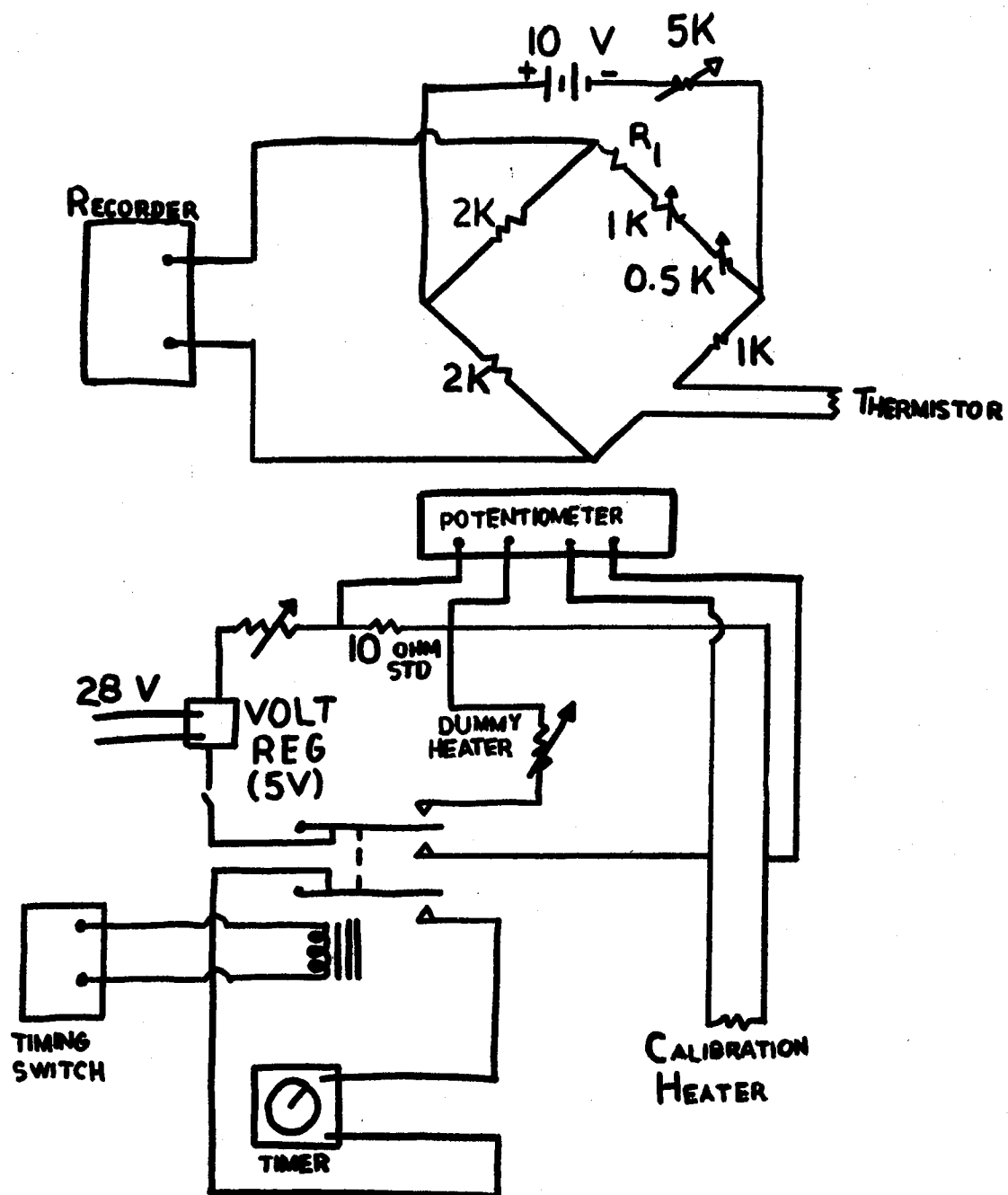


Figure 1. A Schematic Diagram of Temperature Measurement and Calibration Circuits of Calorimeter

bridge of about 1.5 volts would minimize the effects of the change in resistance with voltage, and the reduction in voltage compensated for the increase in sensitivity. Under conditions in which the calorimeters gave the same chart displacement per calorie, the conventional thermistor was significantly noisier. This may be attributable to the effects of greater resistive heating inside the thermistor at the higher voltage (41). The positive temperature coefficient thermistor seemed to offer little advantage, apart from the lower noise level. In both cases, an excellent signal-to-noise ratio was obtained.

Electrical Calibration Circuitry

The electrical calibration circuit is also shown in Figure 1. A constant calibrating voltage is supplied by a battery bank, via the laboratory DC line. Approximately 28 volts is supplied to a Valor Instrument Co. voltage regulator which in turn supplies about 5 volts to the calibration circuit. A decade resistance box, the internal heater, and a 10.00 ohm secondary standard resistor mounted in a Dewar flask are connected in series in the calibration circuit. The decade resistance is adjusted to select the calibration voltage applied to the heater. A second decade resistance which serves as a dummy heater is adjusted to match the resistance of the internal heater and is switched into the circuit between calibrations. A Rubicon Model 2630 potentiometer is used to measure the voltage across the internal heater and the current across the heater is found by measuring the voltage across the standard resistor.

The system is controlled by a timer-switch. The timer-switch is set for an approximate desired length of calibration. When it is

activated, it starts a precision timer to record the exact length of calibration and switches the internal heater into the circuit in place of the dummy heater using a system of relays.

Mechanical System

The mechanical portion of the calorimeter consists of a titration head, glass Dewar flask, temperature control system, and stirrer. These are fabricated so that, except for the platinum heater wire and Teflon titrant delivery needle, the solutions contact only glass.

Figure 2 is a diagram of the titration head of the calorimeter. Part A is the 40 ga. platinum resistance wire which serves as the heater. It is wound around a glass heater support. Part B is the 18 ga. Teflon titrant delivery needle. It is coiled around the bottom of the heater form. It carries a 22 ga. tip, also of Teflon. The smaller tip diameter minimizes mixing of titrant and titrand before the run is begun. The serum-stoppered opening through the needle which enters the calorimeter is labeled C. D is the glass stirrer and E is the thermistor, which is encased in a thin-walled glass tube.

The calorimeter vessels are silvered glass Dewar flasks. The Dewar flasks are fitted with specially constructed water jackets. Constant temperature water is circulated through the jackets by a Haake Type Fe Temperature Controller. The stirrers are powered by Heller Model GT21 motors which are controlled by Cole-Parmer model GT21 Thyraton motor controllers. Titrant is added with a Gilmont Ultraprecision model microliter syringe. Syringes of 2.5 ml and 0.25 ml capacity are used, depending on the volume of titrant which is to be delivered.

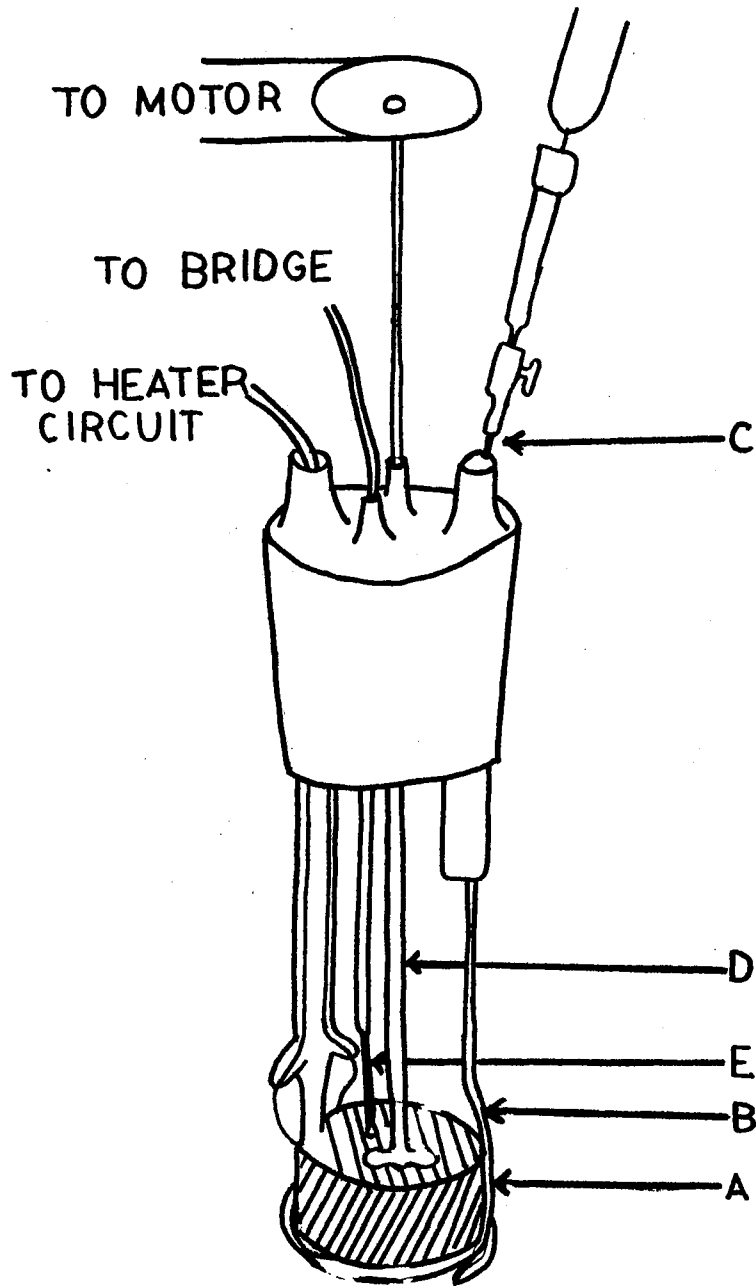


Figure 2. Mechanical Parts of Calorimeter
(See Text for Explanation of Parts
Labelled A-E)

Performance

The performance of each calorimeter was checked by measuring the heat of reaction between NaOH and HCl. This reaction was chosen because it has been extensively studied previously. Multiple runs made on both instruments agreed within less than 1% with each other and with the calorimetrically determined value of -13.46 kcal/mole at 25°C reported by Hale, et al. (42).

Titration Procedure

The Dewar flask is washed and then dried in a vacuum desiccator. The flask is placed loosely around the titration head and purged with nitrogen just prior to filling.

The serum-stoppered bottles containing the working solutions to be titrated are stored in a desiccator. To transfer a sample from the bottle to the calorimeter, either hypodermic syringes or specially constructed transfer pipets equipped with Luer joints are used. The syringe or pipet and a hypodermic needle are dried at least 4 hours in a 125°C oven, then cooled to room temperature by passing nitrogen through them. As the sample is drawn from the bottle, air is introduced through a drying tube filled with Type 4A molecular sieve. The sample is drained into the calorimeter vessel and the vessel is quickly sealed. If a syringe is used, it is weighed both when full and when empty in order to determine the amount of solution transferred. In the case of the pipets, the volume is known from previous calibration by delivery of distilled water.

The filled titration vessel is placed in the temperature jacket and stirred until the system reaches thermal equilibrium. The system is considered equilibrated when the base-line displayed on the chart recorder is judged to be straight and smooth.

The heat capacity of the calorimeter for each run is determined by operating the calibration heater for a measured period of time at a measured voltage and current. The heat capacity in calories per inch of chart displacement is given by

$$C_p = iEt/4.185c \quad (26)$$

where

i - current across the heater in amperes. This can be found by dividing the potential drop across the standard resistor (in volts) by 10.0 ohms.

E - potential drop across the heater in volts

t - length of the calibration run in seconds

c - resultant pen travel in inches

4.185 - joules per calorie

Generally, two heat capacity runs are made before each titration, and two more following. E and i are measured two or three times in each calibration.

The titration is carried out incrementally. The recorder is allowed to establish a straight smooth base line. The increment of titrant is added by quickly turning the syringe micrometer the required amount. A second baseline is then established. The resulting displacement is found by extending the baselines and measuring the distance between them at the mid-point of the addition. (The same procedure is used to determine the displacement in the calibration.) Shown in Figure 3.

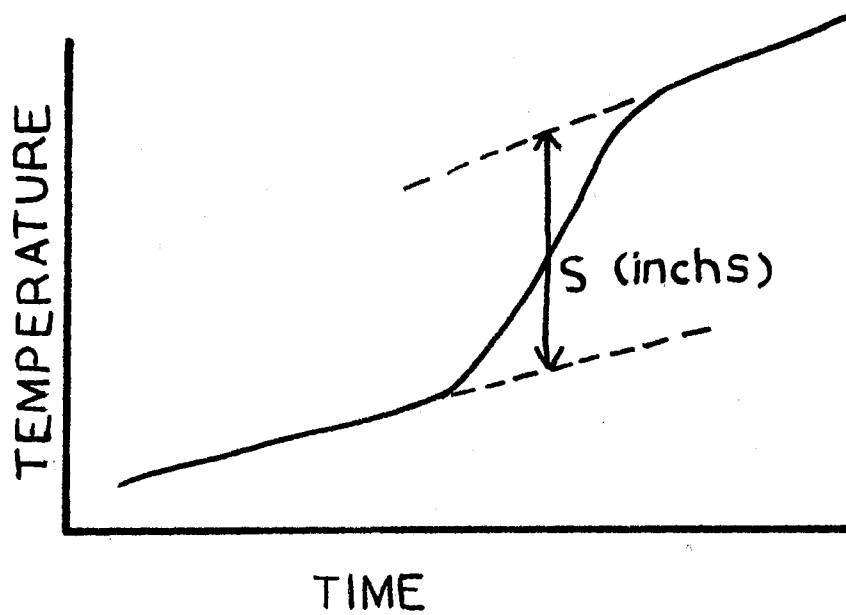


Figure 3. Recording Potentiometer Trace Resulting from Temperature Change Within Calorimeter, with Baseline Extended to Allow Measurement of Attendant Displacement

The titrant delivery needle is coiled around the heater form, immersed in the titrand, so that the increment of titrant in the needle has an opportunity to reach the temperature of the titrand prior to injection. Since the titrand is at room temperature before it enters the needle and the room temperature has been observed to be as low as 23.5°C when a titration was in progress, the maximum allowed increment size is chosen so that the amount of heat required to warm the titrant 1.5°C would be no more than 2% of the expected yield from the addition. A more typical error would be less than 1%, since the sample would at least be partly equilibrated and the room temperature often differs from the vessel temperature by less than 1.5°C , and increments are often smaller than the maximum allowed.

CHAPTER IV

DATA REDUCTION

There are three major steps involved in reduction of the data from recording potentiometer traces to stability constants, stepwise enthalpies of formation, and their error limits. They are 1) measurement of chart displacements, 2) calculation of calories liberated per mole of salt after adding each increment of titrant, and 3) location of the stability constants and enthalpies which best reproduce the data. The direct search procedure is used for step (3), which also generates error estimates. During these steps, corrections are made for resistive heating by the thermistor, heat of stirring, heat leakage from the calorimeter, heat of dilution of the ligand, and nonzero initial ligand concentrations.

Chart Displacements

When an increment of titrant is added to the calorimeter, a temperature change occurs which causes a displacement in the recorder trace. Since the temperature difference between the calorimeter and its surroundings is not the same before and after the addition, the baselines have slightly different slopes which correspond to different heat leakage rates. It is assumed that the leakage rate is linearly proportional to the temperature difference (24). If this is the case, then, the baseline extrapolation method described in Chapter III allows compensation

for the average rate of leakage. The effects of heating due to stirring and power dissipation by the thermistor (resistive heating) are taken to be constant during the time interval in which the addition is made.

Thus, in the process of taking the difference in chart displacements these two effects are canceled out. The same procedure is used to measure the displacement in an electrical calibration.

Calories Per Mole of Salt

A computer procedure has been written to calculate the number of calories liberated per mole of salt present in the calorimeter, as a function of the molarity of the ligand, from input consisting of chart displacements, volumes of ligand added, heat capacities, and total metal concentrations. The procedure, which is in the form of a subroutine (Subroutine FILUP), is described below.

Input to the subroutine consists of the density of the ligand (added as a pure liquid), the molecular weight of the ligand, the heat of mixing for addition of the ligand to pure acetonitrile (also referred to as the heat of dilution of the ligand), the number of runs being processed, and a label for the system being processed. Then, for each calorimeter run, input data consists of the metal concentration, the volume of sample in the calorimeter, the heat capacities before and after the run, the total volume of ligand added, the number of increments of ligand added, and a run label. The initial ligand concentration is also read in. Finally, the chart displacement and titrant volume are read in for each increment.

The heat capacity for an increment is calculated by assuming that the heat capacity during the run varies linearly with volume of titrant

added, and interpolating between the initial and final heat capacities. The chart displacement is multiplied by the interpolated heat capacity to obtain the number of calories liberated in the increment.

The heat liberated is corrected for the heat of dilution of the ligand by subtracting the heat of mixing of the ligand and pure solvent. Since the salt concentration is not altered significantly (because the increments are small relative to the sample volume in the calorimeter), correction for the heat of dilution of the salt solution is neglected.

The net heat liberated is multiplied by the number of moles of salt present in the calorimeter to obtain the heat per mole of salt, and added to the results for the previous increments to produce a running total of the heat per mole of salt. This running total is the Corresponding Solutions Function ($\Delta\bar{H}$).

The Corresponding Solutions Function value and the associated values of C_M and C_L for each data point are stored in an array which is returned to the main program by placing it in COMMON storage. The contents of the array are suitable for further manipulation by most techniques used in coordination chemistry. The printed output includes the contents of this array and the original input data.

Stability Constants and Stepwise Enthalpies

A computer program has been written to calculate the stability constants and stepwise enthalpies of formation for an assumed set of complex formation reactions intended to describe a system investigated by calorimetry. The main program and the subroutine FILUP (described above), ACE, ACEX, CON, FFCT, and DXNV were written by the author. RANDU, DAPLL, and DSINV are part of the IBM System/360 Scientific

Subroutine Package, or SSP, and are documented elsewhere (43). Subroutine DSTR, DRRAY, and DPRD were constructed from SSP subroutines MSTR, ARRAY, and MPRD by declaring necessary variables to be double precision. The main program and FILUP, ACE, CON, and DXNV are documented by listings and flowcharts in Appendix A. Listings of ACEX, FFCT, DSTR, DRRAY, and DPRD are also included.

Main Program

The main program uses the direct search procedure to find a set of stability constants and stepwise enthalpies which minimize U , the error-squared sum. (The significance of minimizing U was discussed in Chapter II.)

The main program calls subroutine FILUP to read in the raw data, and convert it into a form convenient for further manipulation. Additional input consists of information about the number of complexes to be considered, initial estimates of the stability constants, an indication of which coordination reactions are to be considered, and whether any stability constants are to be held fixed during the minimization process. Other input includes a value for the number of stepsizes to be used in the search, and how large each stepsize is to be. (One generally searches the U surface in large steps to find the approximate minimum, then refines this approximation by searching the nearby portion in smaller steps.) The search is then initiated.

Each searching cycle proceeds as follows. Subroutine RANDU is called and returns a random number which is scaled and used to select a stability constant to be varied. The value of the constant is changed by the designated stepsize and ACE is called. ACE returns the calculated

stepwise enthalpies of complexation and the value of U associated with the modified set of constants. If U has decreased, the new value of the constant is retained. Otherwise, the constant is varied in the opposite direction. If this change does not produce a lower U either, the old value of the constant is retained. Then another random number is obtained and another constant is varied. The cycle is complete when all of the constants have been varied. (The procedure is arranged so that no constant is varied more than one turn per cycle and no constant is skipped.)

When a cycle occurs in which no further reduction of U takes place, the search is complete at the stepsize currently being employed. If no smaller stepsize remains to be tried, the main program calculates estimated standard deviations of the stability constants and enthalpies of formation, and the entropy changes associated with the formation of the complexes. (Details of the method used to estimate the standard deviations are discussed later in this chapter.)

Subroutine ACE

Subroutine ACE receives the current values of the logarithms of the stability constants from the main program. ACE uses this information and the results from FILUP, which is in COMMON storage, and returns the set of stepwise enthalpies which corresponds to the given set of constants. This is the procedure ACE follows.

For each ligand concentration, subroutine ACE calls subroutine CON and passes to it the total ligand concentration, total metal concentration, and current values of the logarithms of the stability constants. CON returns the free ligand and free metal concentrations.

ACE uses the free ligand and free metal concentrations at the k^{th} data point of a calorimeter run to calculate the fraction of the total metal concentration, α_n , which is present in the solution as ML_n according to the relation

$$\alpha_{nk} = (\beta_n [M]_k [L]_k^n) / C_{Mk} \quad (27)$$

The α_{nk} values are related to the overall enthalpies of formation of the complexes, h_n by

$$\Delta \bar{H}_k = \sum_{n=1}^N (\alpha_{nk} h_n) \quad (28)$$

at the k^{th} point, where $\Delta \bar{H}_k$ is the heat evolved per mole of salt from $C_L=0$ to C_{Lk} . (That is, $\Delta \bar{H}_k$ is the value of the Corresponding Solutions Function at the k^{th} point.) N is the number of ligand molecules bound to the metal ion in the highest-order complex considered in the model. If C_L is not initially zero, then $\Delta \bar{H}_k$ at each data point in the run will be in error by a constant amount equal to the heat evolved going from $C_L=0$ to the true initial value. This error can be corrected by subtracting Equation 28 for the first data point in the run from the same expression written for the k^{th} data point. The result is

$$\Delta \bar{H}_k - \Delta \bar{H}_1 = \sum_{n=1}^N (\alpha_{nk} - \alpha_{n1}) h_n \quad (29)$$

or

$$\Delta(\Delta \bar{H}_k) = \sum_{n=1}^N \Delta \alpha_{nk} h_n \quad (30)$$

The new set of equations are still linear in h_n , so conventional linear least squares methods can be used to find the values of h_n . ACE calculates $\Delta(\Delta \bar{H}_k)$ and $\Delta \alpha_{nk}$ for each data point and stores the results in COMMON.

A system of equations like Equation 30 may be solved by solving the matrix equation

$$A \cdot HS = DH \quad (31)$$

where A is an N x N symmetric positive definite matrix with elements

$$A_{nn'} = \sum_{k=1}^M \Delta\alpha_{nk} \cdot \Delta\alpha_{n'k} \quad (32)$$

and where DH is an N-dimensional vector with elements

$$DH_n = \sum_{k=1}^M \Delta(\Delta\bar{H}_k) \cdot \Delta\alpha_{nk} \quad (33)$$

and where HS_n is the n^{th} unknown, h_n . The quantity M is the number of experimental data points to which the model is being fitted. ACE uses the SSP subroutine DAPLL to construct A and DH. DAPLL in turn calls FFCT to look up the values of $\Delta(\Delta\bar{H})_k$ and $\Delta\alpha_{nk}$ which were calculated by ACE and stored in COMMON.

One method of solving Equation 31 is to invert A (obtaining A^{-1}). Standard matrix manipulation gives

$$A \cdot HS = DH \quad (34)$$

$$A^{-1} \cdot A \cdot HS = A^{-1} \cdot DH \quad (35)$$

and since $A^{-1} \cdot A = I$,

$$I \cdot HS = A^{-1} \cdot DH \quad (36)$$

$$HS = A^{-1} \cdot DH \quad (37)$$

ACE calls DXNV to invert A and then calls DPRD to evaluate A^{-1} . DH, giving as the result the desired stepwise enthalpies of formation, h_n .

The error-squared sum, U, is calculated by

$$U = \sum_{k=1}^M (\Delta\bar{H}_k - (\sum_{n=1}^N \Delta\alpha_{nk} h_n))^2 \quad (38)$$

and the values of U and the h_n 's are returned to the main program.

One special feature of ACE, the ability (in connection with FILUP, which reads in the data) to deal with nonzero initial values of C_L merits further comment. Nonzero initial values of C_L may arise in several ways. If water is the ligand, it may prove impossible to prepare a sample which is completely anhydrous. If there is leakage from

the titrant delivery tip during the pre-titration equilibration period, the heat evolved upon the first addition will be less than the full amount which should be observed.

In addition to such unavoidable cases, it may be desired to treat only part of the data set. This situation arises if the first one or more stability constants are too large to be determined accurately by calorimetry. Rather than allowing inaccurate values which are artifacts of the calculational method to introduce error into the later constants, it may be desirable to adopt the assumption that at some C_L which is equal to an integral multiple of C_M , say $j \cdot C_M$, the j^{th} complex, ML_j is the single predominant metal-containing species and the net free ligand concentration is very nearly zero. One can then enter an initial value of C_L equal to $-j \cdot C_L$ to compensate for the quantity of ligand which was consumed informing ML_j , and remove the data cards for the increments up to this point. In this case, we may define a new stability constant β_n^* which is

$$\beta_n^* = [ML_n] / [ML_j] [L]^{n-j} \quad (39)$$

This is related to the original β_n by the expression

$$\beta_n^* = \beta_n / \beta_j \quad (40)$$

and thus

$$\beta_n^* = \prod_{i=j+1}^n K_i \quad (41)$$

and

$$K_n = \beta_n^* / \beta_{n-1}^* \quad (42)$$

As a small but important practical point, the program labels the $j+1^{\text{th}}$ constant, $\log \beta_{j+1}$, as $\log \beta_1$, but the value of j can be stated the system label, which is read in alphamerically, thus indicating the actual case.

The ability to introduce a nonzero initial value for C_L increases the variety of models which can be handled by the program.

Subroutine ACEX

Subroutine ACEX receives values of the $\log\beta_n$'s and the h_n 's from the main program. It uses CON to calculate the free ligand and free metal concentrations for each data point. It then calculates values of $\Delta(\Delta\bar{H}_k)$ and $\Delta\alpha_{nk}$ and calculates U for the model, and returns this U to the main program. ACEX is exactly like ACE, except that it uses h_n 's supplied by the main program instead of calculating them.

Subroutine CON

Subroutine CON uses the Newton-Raphson (33) approach to calculate the values of [M] and [L] from C_L and C_M . To find a root of a function $G(x)$, with a derivative $G'(x)$, which is nonzero, the Newton-Raphson procedure is to make some initial approximation to x and refine it by

$$x_i = x_{i-1} + \frac{G(x_i)}{G'(x_i)} \quad (43)$$

CON uses the initial approximation

$$[L] = C_L / (C_M \cdot \beta_1) \quad (44)$$

and then approximated [M] by

$$[M] = C_M / (1 + \sum_{i=1}^N \beta_i [L]^i) \quad (45)$$

Then, CON evaluates G and G'

$$G = [L] + \sum_{i=1}^N i\beta_i [L]^i [M] - C_L \quad (46)$$

$$G' = 1 + \sum_{i=1}^N \{(i)^2 \beta_i [M] [L]^{i-1}\} \quad (47)$$

and finds a new approximation

$$[L]_{\text{new}} = [L]_{\text{old}} + \frac{G([L]_{\text{old}})}{G'([L]_{\text{old}})} \quad (48)$$

The test for convergence is that

$$\frac{[L]_{\text{new}} - [L]_{\text{old}}}{[L]_{\text{old}}} \leq 0.001 \quad (49)$$

and control is returned to ACE when this test is met, or when more than 300 iterations have failed to produce convergence. (In this case, an error message is returned to ACE.)

Subroutine DXNV

Subroutine DXNV is used to calculate the inverse of the coefficient matrix, A^{-1} , as required by subroutine ACE. When the elements of a matrix differ in size by several orders of magnitude, as happens to be the case, the matrix is said to be ill-conditioned (44). Ill-conditioned matrices are difficult to invert. Elimination methods, such as the Gauss elimination or Gauss-Jordan elimination, may give only a poor approximation of the true inverse, even when the inversion is done in double precision arithmetic. Conventional iterative methods such as Gauss-Seidel are frequently difficult to apply, unless the matrix to be inverted is sparse (has many nondiagonal elements equal to zero). DXNV uses Hotelling's method, as described by McCalla (44), to obtain a better approximation of the inverse, beginning with the approximate inverse calculated by subroutine DSINV (43).

E_k , an error matrix, is calculated by subtracting the product of A and the k^{th} approximation of its inverse, D_k , from the identity matrix, I , as $E_k = I - AD_k$, and using E_k the improved inverse, D_{k+1} , can be

calculated. The test for convergence is that the absolute value of no element of E_{k+1} is greater than 0.001. If the method does not converge in 20 iterations, an error message is written out.

Subroutine FFCT

Subroutine FFCT is used by DAPLL to look up values in common storage for use in forming the coefficient matrix, A. FFCT is also used by ACE and ACEX to find values for the calculations of U.

Error Limits

Estimates of the error associated with the reported value of measured or calculated quantities are generally reported in terms of the standard deviation. Nagano and Metzler (45) give the expression

$$\sigma_v = \left(\frac{2U_{\min}}{\text{D.F.} (\partial^2 U / \partial v^2)} \right)^{1/2} \quad (50)$$

for the standard deviation of some variable v , where U_{\min} is the minimum value of the error squared sum, D.F. is the number of degrees of freedom associated with the system, and $\partial^2 U / \partial v^2$ is the second partial derivative of U with respect to v . The number of degrees of freedom in the present study is taken to be

$$\text{D.F.} = (\text{number of data points}) - (2N) \quad (51)$$

where N is the number of complexes considered and there are two constraints (a $\log \beta_n$ and an h_n) associated with each complex.

A difficulty often arises, in that when some of the variables are not linearly related to U , one may not know the functional form of $\partial^2 U / \partial v^2$. In such cases (as the present case) Sillen (29) has suggested assuming that the functional relationship between U and v is a parabola.

While this is not the true functional form, it should approximate the true form near U_{\min} . This is the procedure which was adopted. The h_n 's were linearly related to U , but since some of the variables were not, it was thought best to use this approach in calculating the probable deviations associated with all of the variables. In this way, although the deviations are only approximate, they are calculated in a consistent manner.

CHAPTER V

RESULTS AND DISCUSSION

Titration calorimetry was used to study the interaction between selected trivalent lanthanide perchlorates and water and DMSO in acetonitrile solutions. A computer program was written which calculates the logarithms of the stability constants and the stepwise enthalpy and entropy changes which best reproduce the experimental data, based on a model which is specified by the user at execution time. The thermodynamic quantities so calculated are rationalized in terms of the physical properties of the rare earth ions.

Heats of Mixing of Ligands and Acetonitrile

The heat of mixing of water with acetonitrile was measured by incrementally adding water to dried acetonitrile, following the procedure set forth in Chapter III. Over the range of water concentration from 1×10^{-3} M (present in the dried solvent), to over 1 M, the heat of mixing is observed to be endothermic. The value is constant over approximately the first one-third of this range, and becomes slightly less endothermic over the remainder. On the basis of two titrations to 1 M final concentration and four additional runs covering only the linear region up to about 0.3 M, the heat of mixing in the linear region was found to be +1855 calories per mole, with a standard deviation of ± 13 calories for the six runs. The titrations of the metal ions were

carried out in the linear region.

The heat of mixing of DMSO with acetonitrile was measured in the same manner as for water. The reaction was again endothermic, but was much less so. Two runs gave an average value of +44 calories per mole, with runs differing by about 7 calories per mole. Since this heat was so small as to approach the limits of detection for the calorimeter, and since the value is also small in comparison to the heat evolved when DMSO reacts with a lanthanide ion, it was considered unnecessary to attempt further refinement of this result.

The larger heat of mixing for water as compared to DMSO reflects the fact that in liquid water the protons of each water molecule hydrogen bond strongly to the oxygen of its neighbors. The breaking of these bonds which occurs when water dissolves in acetonitrile is endothermic and is not completely compensated by the forming of bonds between water and acetonitrile. By comparison, the methyl protons of DMSO should be involved in hydrogen bonding to a much smaller extent.

Metal-Ligand Titrations

Five metals from the lanthanide series were chosen for study. La, Nd, Gd, Ho, and Lu were selected because they span the series and their tripositive ions have fairly regularly spaced values of reciprocal ionic radius ($1/r_{\text{ion}}$). In addition, La^{+3} , Gd^{+3} , and Lu^{+3} have $4f^0$, $4f^7$, and $4f^{14}$ configurations, and would exhibit no ligand field effect. Nd^{+3} and Ho^{+3} have $4f^3$ and $4f^{10}$ configurations, and would have equivalent ligand-field stabilization energies. Working solutions were prepared of approximately 0.060 M, 0.045 M, 0.030 M, and 0.015 M in the case of La^{+3} and Nd^{+3} , 0.060 M and 0.015 M in the case of Ho^{+3} and Gd^{+3} , and 0.025 M

and 0.015 M in the case of Lu^{+3} . It was desired to span a reasonable concentration range without having the lower limit so low that it would be difficult to reproduce the data, or the upper limit being so high that the solutions could not be safely prepared. (The explosion which occurred during the preparation of these solutions is reported in Chapter III.) The number of concentrations was reduced from four to two after it was found that the Nd and La data sets were so large that the computer processing of the data work took an excessive amount of computer time. (One La model, which happened to involve a particularly large number of stability constants, required almost 50 minutes of CPU time on an IBM 360 Model 65 computer.) The concentration range was narrowed for Lu because of the cost of Lu_2O_3 . Duplicate runs were made at all concentrations. Separate batches of working solution were prepared from the same stock solution for the water and DMSO studies in all cases but Lu. (A single batch of each working solution was prepared in the case of Lu to decrease the amount consumed in routine analysis).

Results from Water Systems

In preliminary experiments, water was added to acetonitrile solutions containing lanthanide perchlorates until the ratio of moles of water per mole of salt reached values as high as 40:1. In no case did the observed quantity of heat evolved approach the heat of mixing previously determined for addition of water to pure acetonitrile. If no other processes were occurring, the heat should approach the endothermic heat of mixing as the metal ion's coordination sites were gradually filled with water molecules instead of acetonitrile molecules. When the sites were all occupied by water, only the heat of mixing would be

observed upon addition of more water to the solution. (One should not take the above statement to mean that all of the coordinated water would necessarily be in the primary coordination sphere of the metal ion when this condition is reached.) Wallace (23) observed a similar effect upon adding water to 1-butanol solutions of transition metal perchlorates. He attributed this behavior to preferential reordering of the metal ion's solvent sheath.

When water is added to a non-aqueous salt solution, water molecules tend to gather around the ions and coordinate with them, displacing solvent molecules in the process. As more and more water molecules collect around the ions, any given water molecule which is near an ion will find itself nearer to other water molecules on the average than it would be in the bulk solution. As the environment near an ion begins to resemble liquid water, water structure will begin to form. The making of hydrogen bonds which is involved in forming such water structure is exothermic, and such an exothermic contribution may be the reason that the observed heat is never as endothermic as when water is added to the pure solvent. Heat of reaction and the heat of mixing cancelled each other and the net temperature change became zero. This corresponds to water-to-metal ratios of from 5:1 to 10:1, depending on the metal and its concentration.

When computer analysis of the data over the entire concentration range for the water titrations was attempted, no model was found which would allow the program to converge on plausible answers. Frequently, the program converged on enthalpies which were on the order of 1,000,000 cal/mole and which had alternating signs. The stability constants were spaced so that as C_L varied, the small difference between

the large enthalpy values produced numbers which fitted the experimental data.

The data sets were then truncated at the first increment which produced a C_L / C_M ratio of 2:1, and the rest of each calorimeter run was removed from the data deck. Models involving formation of from one to four complexes were fitted to this truncated data set. A model assuming the formation of complexes with the compositions ML , ML_2 , and ML_3 gave the best fit. The results for this model are presented in Table II. The reader should note that the lowest value for $\log\beta_1$ is almost 3.90. Thus, the free ligand concentration is always very nearly zero while the first complex is being formed, and the stability constant cannot be determined with great accuracy by calorimetry. The fact that the reaction is essentially quantitative does not impair the determination of the enthalpy change associated with the formation of the first complex, and the values of h_1 are plotted as a function of the ionic radius of the metal ion in Figure 4.

Since the first stability constant is too large to measure accurately, it follows that at C_M equal to C_L , the metal is essentially all in the form of ML . Thus, one can remove the first part of the data set and consider the formation of the later complexes from ML . The program is constructed to provide this option, as was discussed in Chapter IV. The notation introduced at that time refers to the complex which is taken to be the starting point as the j^{th} complex, ML_j . Various models with values of j ranging from 1 to 4 and considering the formation of from 1 to 6 additional complexes were tried for the water data. The model which produced the best fit for each system is presented in Table III.

TABLE II
THERMODYNAMIC RESULTS FOR WATER SYSTEM
CALCULATED FROM TRUNCATED DATA SET

METAL	i	$\log \beta_i \pm \sigma_{\beta_i}$	$\log K_i$	$h_i \pm \sigma_{h_i}$ (kcal/mole)	ΔH_i	s_i (cal/°K)	ΔS_i	% average deviation for model
La	1	4.11 ± .011	4.11	- 4.82 ± .05	- 4.82	+ 2.66	+ 2.66	1.73
	2	5.89 ± .016	1.70	-12.53 ± .08	- 7.71	-15.1	-17.7	
	3	7.84 ± .010	1.95	-16.62 ± .08	- 4.09	-19.9	- 4.8	
Nd	1	3.90 ± .004	3.90	- 5.71 ± .07	- 5.71	- 1.30	- 1.30	2.07
	2	6.10 ± .025	2.70	-11.91 ± .06	- 6.21	-12.1	-10.8	
	3	8.05 ± .004	1.95	-17.73 ± .01	- 5.82	-22.7	-10.6	
Gd	1	3.90 ± .005	3.90	- 5.26 ± .02	- 5.26	- 0.18	- 0.18	2.20
	2	6.10 ± .005	2.20	-11.42 ± .01	- 6.16	-10.4	-10.22	
	3	8.06 ± .009	1.96	-17.13 ± .02	- 5.71	-20.6	-10.2	
Ho	1	3.87 ± .007	3.87	- 5.34 ± .02	- 5.34	- 0.23	- 0.23	2.58
	2	6.12 ± .006	2.25	-12.12 ± .01	- 6.78	-12.7	-12.5	
	3	8.09 ± .009	1.97	-17.52 ± .03	- 5.40	-21.8	- 9.1	
Ln	1	3.90 ± .009	3.90	- 5.37 ± 1.4	- 5.37	- 0.16	- 0.16	3.85
	2	6.08 ± .018	2.18	- 9.75 ± .06	- 4.38	- 4.89	- 4.70	
	3	8.06 ± .016	1.98	-24.36 ± .05	-14.61	-44.8	-39.9	

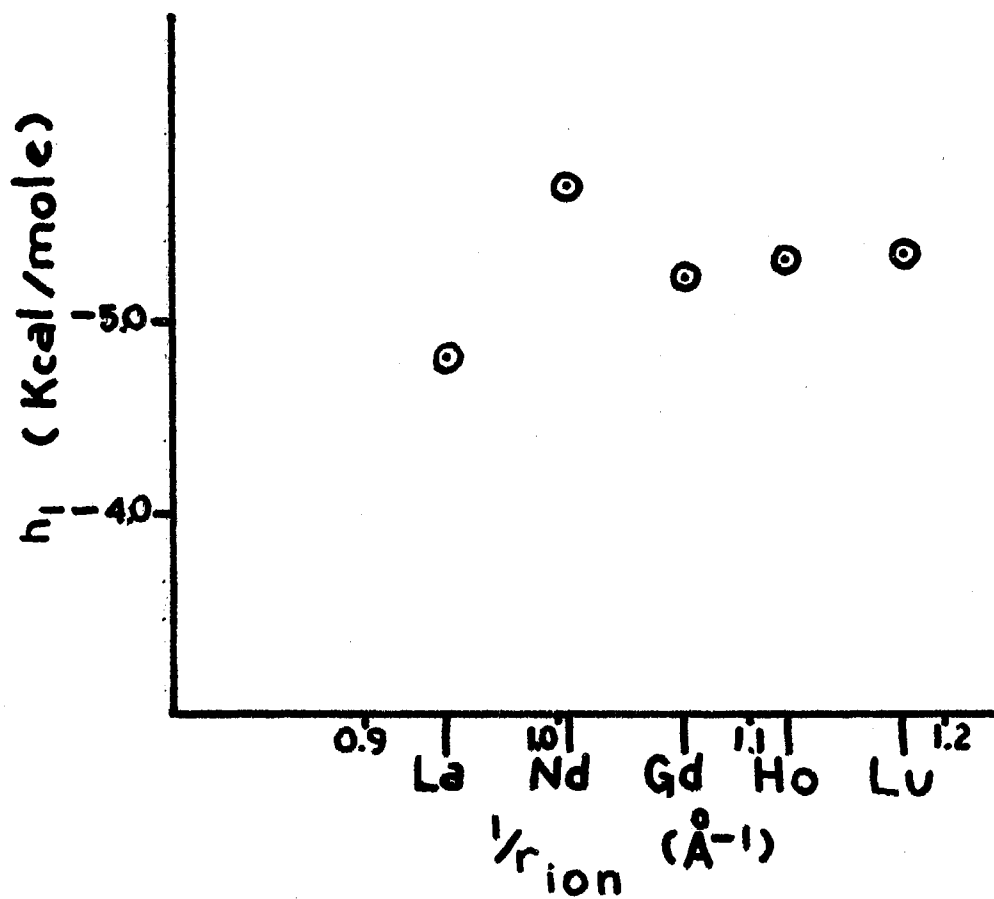


Figure 4. Plot of h_1 as a Function of $1/r_{ion}$ for Water System

TABLE III

THERMODYNAMIC RESULTS FOR WATER SYSTEM
CALCULATED FROM HIGHER ORDER DATA SET

METAL	i	$\log \beta_i^* \pm \sigma_{\beta_i^*}$	$\log K_i$	$h_i^* \pm \sigma_{h_i^*}$ (kcal/mole)	ΔH_i	s_i^* (cal/°K)	ΔS_i	% average deviation for model
La j=1	2	1.99 ± .06	1.99	- 5.51 ± .07	- 5.51	- 9.4	- 9.4	1.73
	3	3.51 ± .06	1.53	-16.7 ± .16	-12.2	- 39.4	- 30.4	
	4	5.24 ± .04	1.73	-12.7 ± .56	+ 4.0	- 18.7	+ 21.2	
	5	5.53 ± .10	0.29	-59.2 ± .34	-46.5	-173.3	-154.6	
	6	6.48 ± .07	0.95	-21.8 ± .22	+37.4	- 43.5	+129.8	
Nd j=3	4	1.82 ± .04	1.82	- 5.30 ± .07	- 5.30	- 9.4	- 9.4	.87
	5	3.76 ± .06	1.94	- 9.45 ± .09	- 4.15	- 14.5	- 5.1	
	6	5.64 ± .05	1.88	- 8.20 ± .04	+ 1.25	- 1.7	+ 16.2	
	7	6.50 ± .06	0.86	-19.7 ± .12	-11.5	- 36.5	- 34.8	
Gd j=3	4	1.98 ± .01	1.98	- 6.52 ± .12	- 6.52	- 12.8	- 12.8	4.44
	5	4.23 ± .01	2.25	- 6.98 ± .14	- 0.46	- 4.1	+ 8.7	
	6	4.83 ± .05	0.60	-23.65 ± 3.2	-16.67	- 57.3	- 53.2	
Ho j=2	3	2.06 ± .06	2.06	- 6.57 ± .07	- 6.57	- 12.6	- 12.6	.45
	4	4.20 ± .04	2.14	-10.56 ± .04	- 3.99	- 16.2	- 3.6	
	5	5.93 ± .03	1.73	-14.65 ± .04	- 4.09	- 22.0	- 3.8	
	6	7.20 ± .06	1.27	-17.71 ± .07	- 3.06	- 26.5	- 4.5	
	7	8.21 ± .05	1.01	-24.16 ± .11	- 6.45	- 43.5	- 17.0	
Lu j=1	2	2.50 ± .04	2.50	- 5.27 ± .04	- 5.27	- 6.23	- 6.23	1.20
	3	3.99 ± .13	1.49	-33.6 ± .64	-28.3	- 94.5	- 78.3	
	4	6.50 ± .05	2.51	-13.8 ± .06	+19.8	- 16.5	+ 68.0	
	5	7.81 ± .05	1.31	-32.9 ± .09	-19.1	- 74.6	- 58.1	

Results from the DMSO System

The complexes formed between DMSO and a given lanthanide ion seem to exhibit a limiting coordination number. As DMSO is added to an acetonitrile solution of a rare earth perchlorate, the first several increments added cause about the same number of calories to be produced per mole of salt in the calorimeter. After a number of increments have been added, the amount of heat evolved begins to decrease, and finally, addition of more DMSO releases no more heat. (At a sensitivity setting appropriate to record the heat produced by the reaction, the heat of mixing of DMSO and acetonitrile is too small to observe.) Figure 5 is a plot of the Ho-DMSO data, which exhibits this behavior.

The shape of the plot suggests that one may obtain some information about the system preliminary to computer analysis. If the reaction occurred quantitatively (that is, if the equilibrium constants were large) and if the coordinated DMSO molecules were equivalent (that is, if attaching three DMSO molecules liberated three times the heat produced by attaching the first one), then the plot of calories liberated per mole of salt versus C_L (as, for instance, Figure 5) would look like Figure 6a. If one makes the extrapolation shown in Figure 6b, then the C_L at which the two extrapolated lines cross $C_{L\text{int}}$ can be used to estimate the limiting coordination number (n_{lim}) if the analytical concentration (C_M) of the salt solution is also available, as given by

$$n_{\text{lim}} = C_{L\text{int}}/C_M \quad (52)$$

Such calculation was performed for the DMSO data. The results are presented graphically in Figure 7, and tabulated in Table IV.

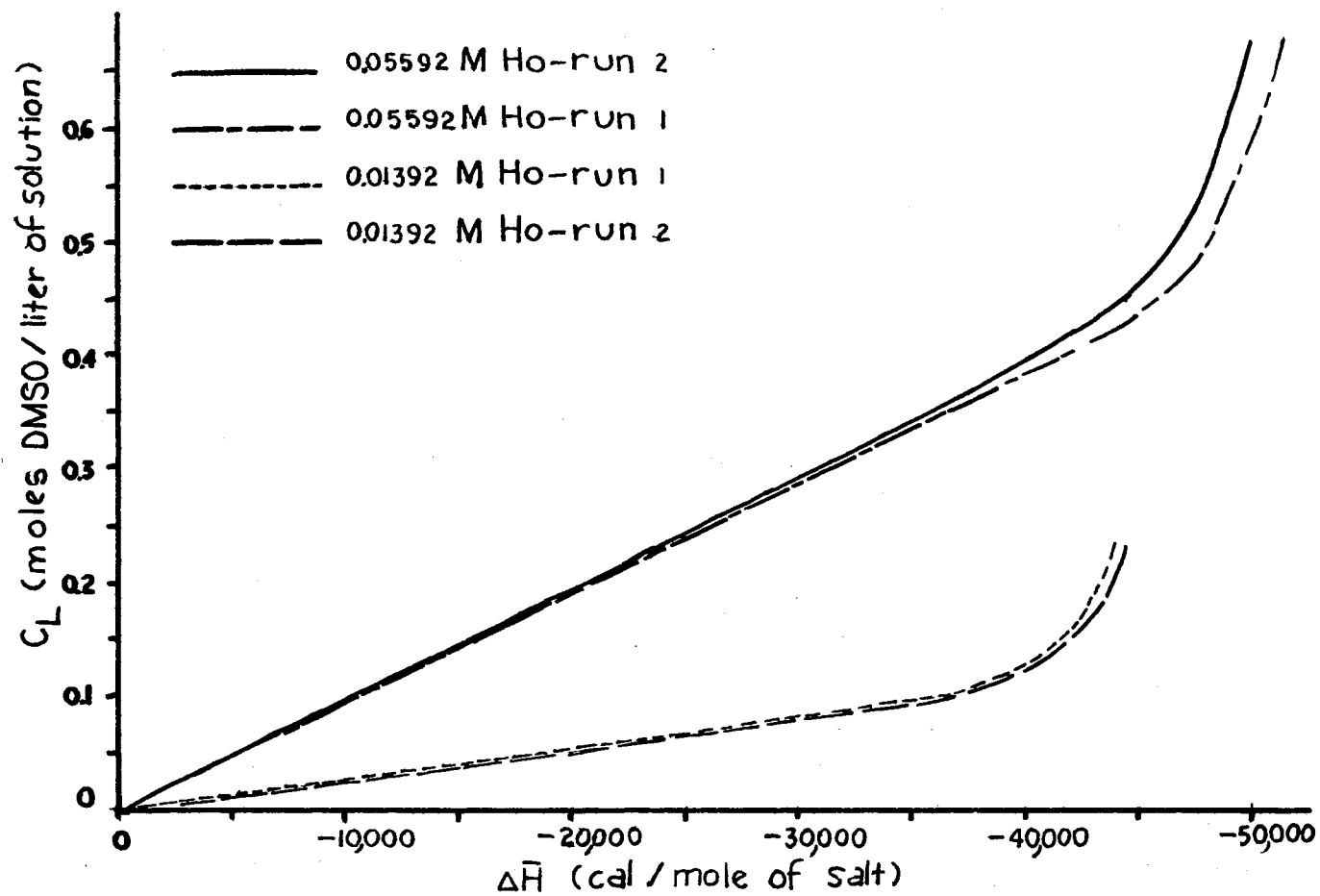


Figure 5. Plot of $\Delta \bar{H}$ as a Function of C_L for Ho-DMSO Titrations

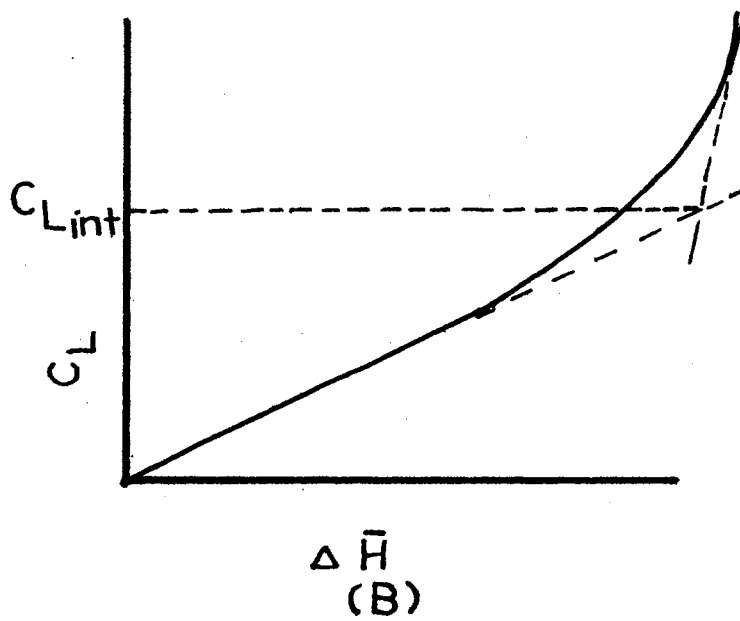
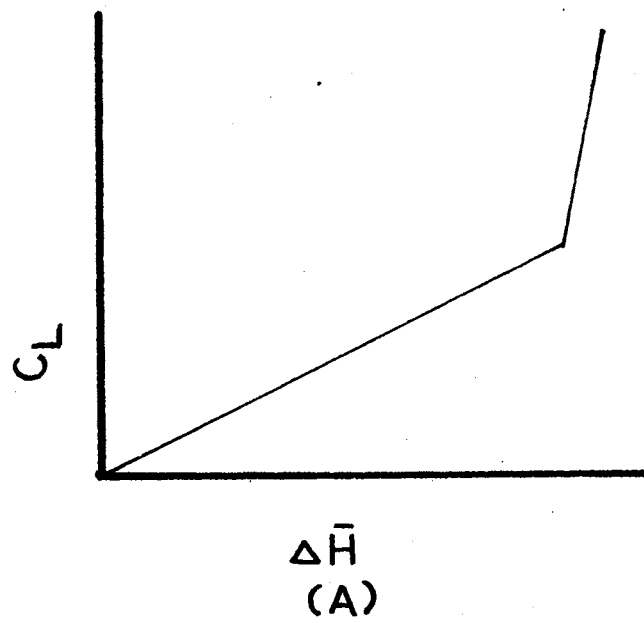


Figure 6. Hypothetical Plots of $\Delta \bar{H}$ as a Function of C_L for the Cases of Complete and of Incomplete Reaction

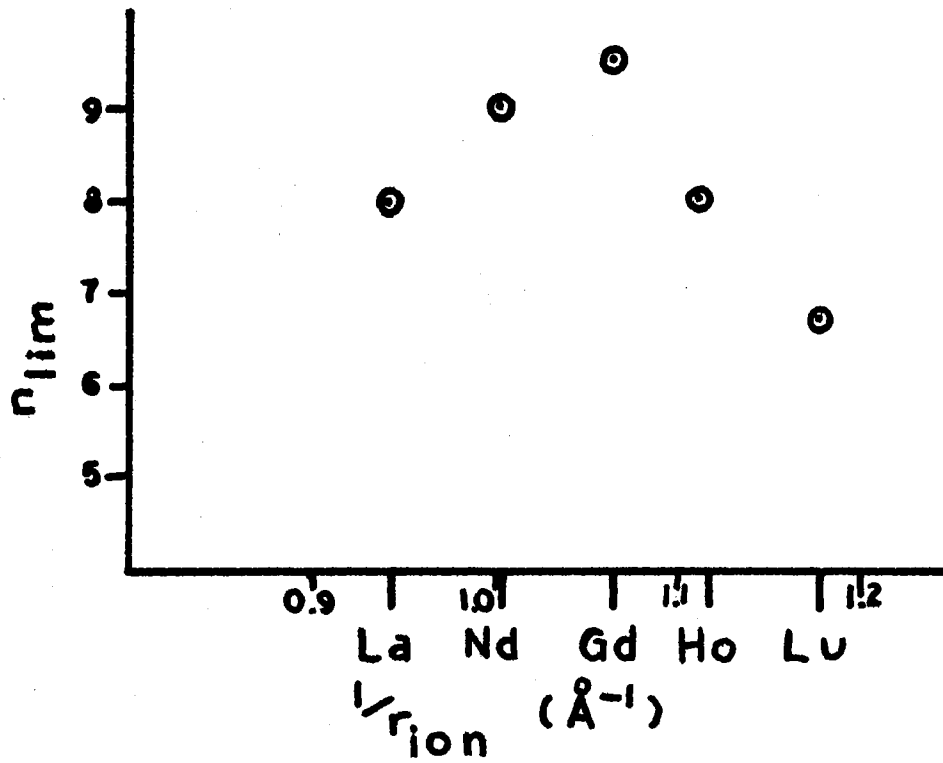


Figure 7. Plot of Graphically Estimated Limiting Coordination Number as a Function of $1/r_{ion}$

TABLE IV
 GRAPHICALLY ESTIMATED AND NUMERICALLY CALCULATED
 LIMITING COORDINATION NUMBERS

Metal	n_{lim} computed	K_n	α_9 computed	n_{lim} graphical
La	9	2.5	0.065	8.0
Nd	9	17.4	0.175	9.0
Gd	9	20.9	0.276	9.6
Ho	8	13.5	-----	8.0
Lu	7	126.0	-----	6.7

One can also use a plot like the one shown in Figure 5 to estimate the magnitude of the stability constants which are not too large to be evaluated calorimetrically and to identify the ones which are likely to prove too large to measure. Assume that at the C_L value of $(n + 0.5) \cdot C_M$, the only reaction one need consider to be occurring is



for which the equilibrium constant, K may be written

$$K_{n+1} = [ML_{n+1}] / [ML_n] [L] \quad (54)$$

Further assume that at $C_L = (n + 0.5) \cdot C_M$ one may write

$$[ML_{n+1}] = [ML_n] \quad (55)$$

and thus

$$K_{n+1} = 1 / [L] \quad (56)$$

The deviation of the plot gives the free ligand concentration. As shown in Figure 8, one follows the extrapolated line to $C_L = (n + 0.5) \cdot C_M$ and moves vertically to the true curve. The C_L value at which one intersects

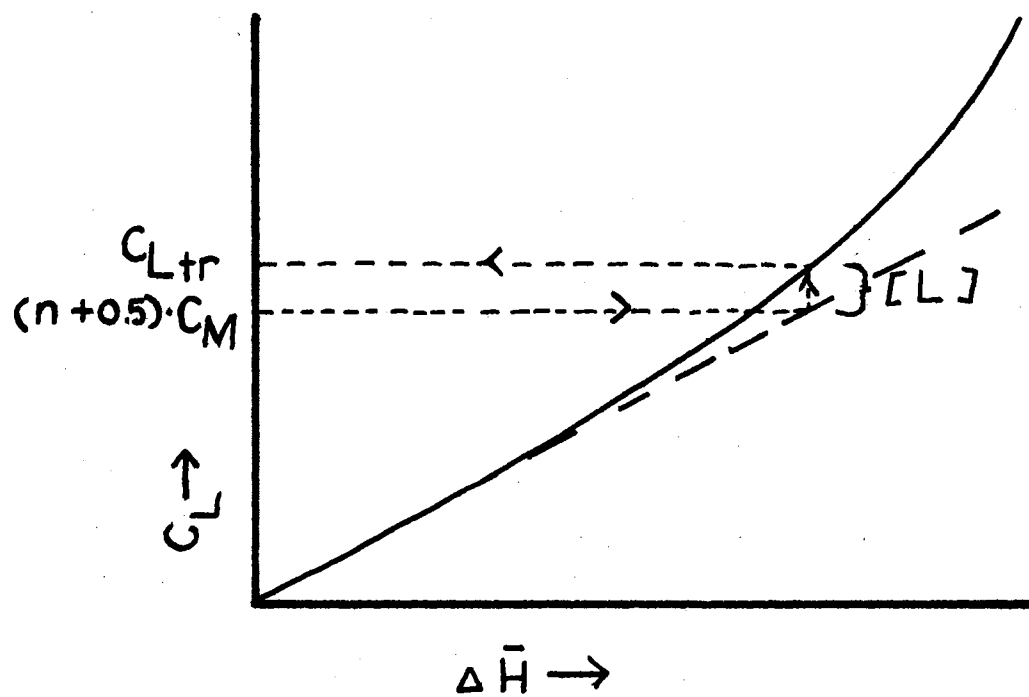


Figure 8. Use of Plot of $\Delta \bar{H}$ vs $1/r_{ion}$ to Estimate the Free Ligand Concentration, $[L]$ at Some Value of C_L

the true curve, C_{Ltr} is then used to find $[L]$

$$[L] = C_{Ltr} - (n + 0.5) \cdot C_M \quad (57)$$

For the above set of assumptions to be valid, K_n and K_{n+2} should differ from K_{n+1} by two orders of magnitude, or the K 's above and below the region of interest must at least vary symmetrically, but even if the answer is not rigorously correct, it provides a useful initial guess for use in the computer program. If the actual curve does not deviate from the extrapolated straight line, the complex is too stable for the determination of the stability constant by calorimetry.

A third use of a plot like Figure 5 is to estimate the enthalpy of formation for the first complex. At very low concentrations, one may assume that only the first complex is being formed significantly. If this is correct, then the initial slope is equal to ΔH_1 , the enthalpy of formation of the first complex. Again, even though the assumption may not be completely valid if the reaction is not quantitative, it provides some idea of what value to expect from the computer program.

As in the case of the water system, no model would fit the entire range of data and give reasonable answers, so the data set was again truncated at the first point in each run at which C_L/C_M exceeds 2:1. The first β_n 's are again too large to determine with accuracy. The results of this computation are presented in Table V, along with the initial slope estimates of ΔH_n , which are placed in parentheses below the computer-calculated values. These are plotted in Figure 9.

Since the first few β_n 's were too large to be determined, the assumption was again adopted that some complex ML_j was formed quantitatively at $C_L = j \cdot C_M$ and that further complexes were formed from this starting point. The values calculated for the model which best fit each

TABLE V
THERMODYNAMIC RESULTS FOR DMSO SYSTEM
CALCULATED FROM TRUNCATED DATA SET

METAL	i	$\log \beta_i \pm \sigma_{\beta_i}$	$\log K_i$	$h_i \pm \sigma_{h_i}$ (kcal/mole)	ΔH_i	s_i (cal/°K)	ΔS_i	% average deviation for model
La	1	7.75 ± .02	7.75	- 6.05 ± .04 (-6.25)*	- 6.05	+15.1	+15.1	2.58
	2	8.85 ± .04	1.10	-35.4 ± 1.9	-29.35	-78.5	-93.6	
	3	12.6 ± .01	3.80	-17.9 ± .09	+17.5	- 2.30	+76.2	
Nd	1	6.95 ± .02	6.95	- 5.01 ± .15 (-5.17)*	- 5.01	+15.0	+15.0	4.52
	2	9.45 ± .11	2.50	-11.3 ± .55	- 6.29	+ 5.32	- 9.68	
	3	12.9 ± .03	3.45	-14.9 ± .18	- 3.6	+ 8.84	+ 3.52	
Gd	1	7.30 ± .01	7.30	- 4.86 ± .10 (-4.63)*	- 4.86	+17.1	+17.1	2.23
	2	9.35 ± .06	2.05	- 5.88 ± .61	- 1.02	+23.1	+ 6.0	
	3	12.9 ± .01	3.55	-16.9 ± .09	-11.02	+ 2.15	+20.95	
Ho	1	6.85 ± .01	6.85	- 5.94 ± .03 (-5.85)*	- 5.95	+11.4	+11.4	1.32
	2	10.1 ± .01	3.25	-12.1 ± .10	- 6.16	+ 5.35	- 6.05	
	3	12.7 ± .03	2.60	-19.0 ± .13	- 8.9	- 5.62	-10.97	
Lu	1	7.95 ± .03	7.95	- 6.44 ± .15 (-6.21)*	- 6.44	+14.8	+14.8	1.12
	2	9.19 ± .08	1.24	-28.2 ± .03	-21.8	-52.6	-67.4	
	3	12.6 ± .04	3.41	-19.2 ± .13	+10.0	- 6.7	+45.9	

* the quantity in parentheses below the value for h_i calculated by the computer is the initial slope value

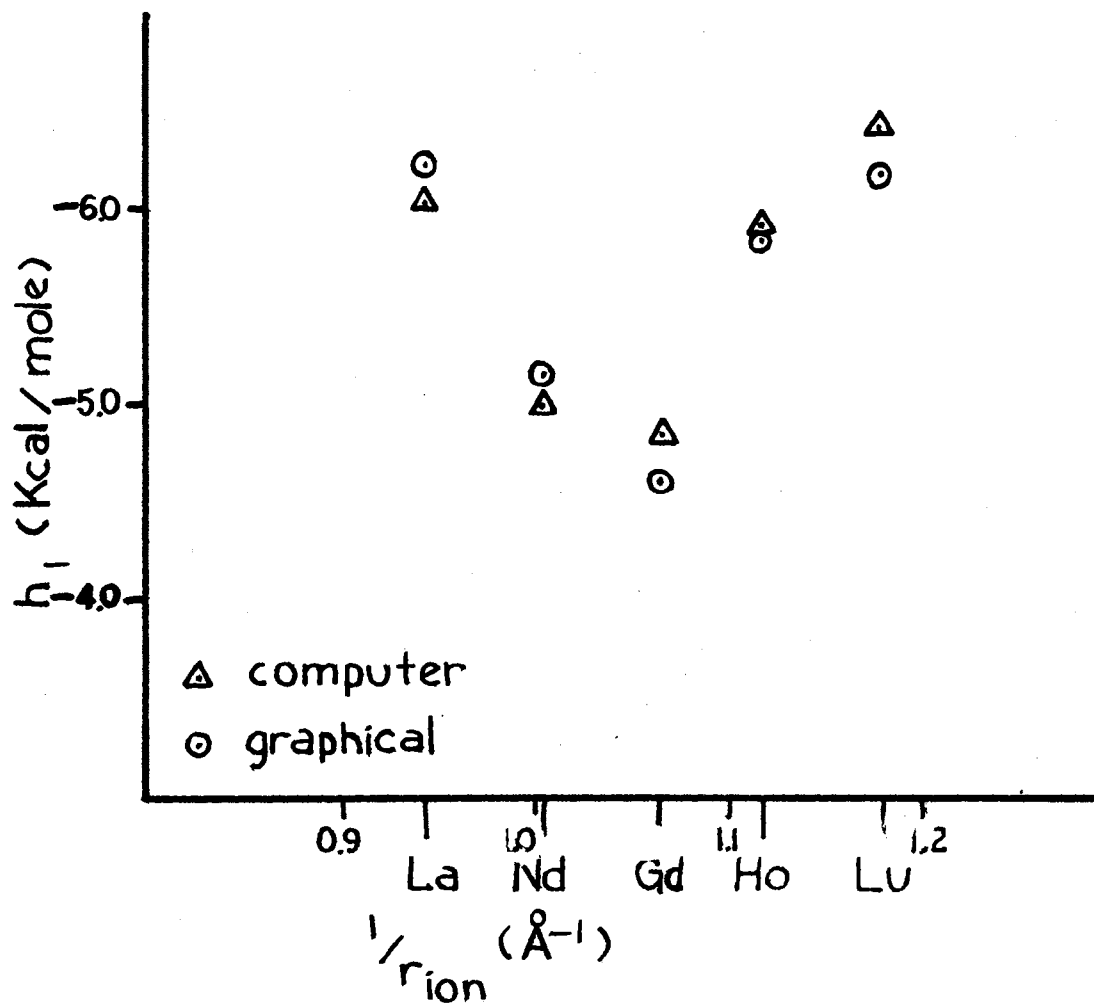


Figure 9. Plot of h_1 as a Function of $1/r_{ion}$ for DMSO System

data set from the DMSO system are listed in Table VI. The values of n and K_n calculated for the highest order complex considered in each "best" model are tabulated in Table IV.

The first three metals studied, La, Nd, and Gd formally appear to have the same limiting coordination number. However, when the values for K_9 are considered, it appears that in terms of how many DMSO molecules one would expect to find attached to each metal ion, on an average, the number would increase from La to Nd to Gd. Subroutine CON was used to calculate $[M]$ and $[L]$ from the best set of stability constants for these three metals. C_M was assumed to be 0.030 M and the C_L/C_M ratio was taken as 9:1. Values for α_9 , the fraction of total metal ion content present in the form of ML_9 , were calculated from Equations 14 and 17, and included in Table IV. These values also indicate that the average maximum coordination number increases from La to Nd to Gd. In the latter half of the series, however, this trend is reversed. For Ho, the species ML_9 need not be considered at all in order to reproduce the data, and for Lu, neither ML_8 or ML_9 are needed. This supports the general trend first indicated by the graphical method.

Discussion of Standard States and Activities

Christensen and Izatt (46) have pointed out the lack of a universally accepted standard state to which solution calorimetric measurements may be referred. They suggest that a temperature and pressure of 25°C and 1 atm be used. They advocate an ionic strength of zero and propose that concentrations be based on either the molarity or mole fraction scale.

The choice of zero ionic strength as the standard state merits

TABLE VI
THERMODYNAMIC RESULTS FOR DMSO SYSTEM
CALCULATED FROM HIGH ORDER DATA SET

METAL	i	$\log \beta_i^* \pm \sigma_{\beta_i^*}$	$\log K_i$	$h_i^* \pm \sigma_{h_i^*}$ (kcal/mole)	ΔH_i	s_i^* (cal/°K)	ΔS_i	% average deviation for model
La j=6	7	1.89 ± .002	1.89	- 8.18 ± .05	- 8.18	-18.8	-18.8	4.03
	8	4.51 ± .001	2.72	-11.1 ± .11	- 2.92	-16.5	+ 2.3	
	9	4.90 ± .002	0.39	-24.6 ± .16	-13.5	-60.1	-43.6	
Nd j=7	8	2.04 ± .13	2.04	- 5.59 ± .18	- 5.59	- 9.42	- 9.42	5.49
	9	3.28 ± .12	1.24	- 9.34 ± .17	- 3.75	-16.3	- 6.88	
Gd j=6	7	2.43 ± .05	2.43	- 5.83 ± .09	- 5.83	- 8.44	- 8.44	1.62
	8	4.11 ± .09	1.68	-13.7 ± .11	- 7.87	-27.2	-18.8	
	9	5.43 ± .11	1.32	-16.3 ± .08	- 2.60	-29.7	- 2.5	
Ho j=5	6	3.05 ± .05	3.05	- 6.61 ± .06	- 6.61	- 8.22	- 8.22	2.28
	7	6.14 ± .06	3.09	-11.7 ± .10	- 5.09	-11.1	- 2.88	
	8	7.27 ± .42	1.13	-24.4 ± .12	-12.7	-48.6	-37.5	
Lu j=5	6	2.46 ± .07	2.46	- 4.66 ± .23	- 4.66	- 4.38	- 4.38	4.37
	7	4.56 ± .12	2.10	-16.2 ± .19	-11.5	-33.5	-29.12	

additional comment. Experiments are frequently done in a medium of constant ionic strength by adding a large, fixed concentration of some presumably inert electrolyte. However, even if the electrolyte does not interact directly with the substance under study, it competes with the substance for solvent molecules. Thus, such results are dependent on the electrolyte chosen. The use of zero ionic strength as the standard state avoids this limitation.

As it was pointed out in Chapter II, activity corrections were neglected in the present calculations. The Debye-Hückel theory was not considered applicable to experiments done in a non-aqueous solvent such as acetonitrile. In addition, uncertainty about the degree of ion association, precluded reliable calculation of the ionic strength.

However, it should be noted that the calculated formation constants and enthalpies of formation fit the experimental data over a fourfold concentration range (from 0.015 M to 0.060 M). This indicates that the values are not too dependent on concentration. Wallace (23) reported that the conductance behavior of the divalent transition-metal perchlorate in 1-butanol is indicative of essentially complete ion association in the concentration range from approximately 0.01 M to 0.10 M. If the trivalent lanthanide perchlorates are similarly predominantly unionized in acetonitrile, then the ionic strength of the solutions approaches zero and the activity coefficients approach unity as the standard state is reached. This would be consistent with the apparent lack of concentration dependence of the $\log K_n$'s and ΔH_n 's. If this is indeed the case, then the values reported here for ΔG , ΔH , and ΔS can be equated with ΔG^0 , ΔH^0 , and ΔS^0 . If this is not the case, the reported values are conditioned. Since all of the experiments were carried out under

similar conditions, they may properly be compared internally in any case. The temperature of 25°C, pressure of 1 atm, and molar concentrations were used in accord with the previously cited recommendations.

Discussion of Factors Affecting Complex Stability

The tripositive lanthanide ions are generally considered to be quite similar chemically. The simplest attempts to explain their coordination behavior, as was mentioned in Chapter I, have generally predicted monotonic increases in stability across the series as the decreasing ionic radius enhanced the coulombic interaction. The deviations from this simple pattern have been attributed to changes in hydration or solvation number. These changes were often rationalized in terms of steric hindrance.

Karraker (18) has remarked that the best approximation of lanthanide coordination geometry in solution is probably a sphere. This viewpoint is consistent with the evidence that the 4f orbitals probably do not participate to any major extent in bonding in lanthanide compounds (2). If this picture is accurate, then for monodentate ligands, there should be less surface area and hence fewer coordination sites available as the ion size decreases.

The result is that two opposing forces are at work. With successively smaller ions, the enhancement of the coulombic forces causes a larger fraction of the available coordination sites to be occupied. This causes the average coordination number to increase early in the series. But with smaller ions, the steric effect gradually begins to reduce the number of sites which are potentially available, and later in the series the decreasing site availability outweighs the enhanced

probability of site occupation. This explanation is sufficient to account for the maximum observed in the apparent limiting coordination number for the DMSO complexes near the middle of the lanthanide period. There are other observations which are more difficult to explain.

In the simplest possible case, the enthalpies of formation for the successive complexes should be approximately equal for a given metal. Each of the ligand-metal bonds should be equivalent, and hence equally strong. The successive entropies of formation should also be equal. Each reaction involves one mole of ML_{n-1} and one mole of L combining to form one mole of ML_n . This process involves a loss of one mole of particles and their associated degrees of freedom, and the increase in the order of the system should have associated with it a characteristic decrease in entropy which should not depend on the detailed nature of ML_n . The successive K_n 's should decrease because each species ML_n has fewer vacant coordination sites than the preceding ML_{n-1} and thus the additional molecules of L have a smaller statistical chance of finding an unoccupied site and forming ML_{n+1} .

If one examines the successive enthalpies, entropies, and equilibrium constants for complex formation reported in this study, in no case does one observe the simple trends listed above for a given metal-ligand pair. This is because the description in the preceding paragraph is oversimplified. No consideration is made of the solvent molecules surrounding the metal ion, which compete with the ligand for coordination sites. There are two basic patterns in which this solvent-ligand competition can be grouped.

The ligand may displace a solvent molecule from the metal ion's coordination sphere. The observed enthalpy change associated with this

process is the difference between the enthalpy associated with attaching a mole of ligand molecules to a mole of metal ions (or some species ML_{n-1}) and the enthalpy associated with attaching a mole of solvent to the metal. The entropy change in the process should be nearly zero, since a mole of free solvent replaces a mole of free ligand in the solution.

The ligand may, on the other hand, squeeze itself into the metal's coordination sphere without displacing a solvent molecule. If the solvent molecules are loosely attached or uncrowded enough for this to happen, the enthalpy change will be just that associated with binding a mole of ligand to a mole of metal ions. The entropy change in this case will be relatively large and negative, as no solvent molecules are freed to compensate for the loss of free ligand.

In fact, no given actual reaction is likely to fit cleanly into one or the other category. It is an oversimplification to regard either solvent or ligand molecules as being either completely free to translate within the solution or as being perfectly rigidly bound to the metal ion. In the displacement (or substitution) process, the solvent molecule may not be completely expelled from the metal ion's influence. It may, for example, move from the first to the second coordination sphere. In the addition process, the rearrangement of solvent and previously attached ligand molecules may involve some weakening of previously formed bonds. Even so, the addition of a given ligand to a given metal species in solution may resemble one process more than the other. The detailed relationship between successive K_n 's will depend on how the two limiting processes contribute to the actual case, since value of K_n is a function of the free energy and involves both enthalpy and entropy contributions.

R. E. Powell (47) has reported values of 14 e.u. and 28 e.u. respectively for the translational entropy of a non electrolyte dissolved in water and in benzene. The solvent properties of acetonitrile should lie somewhere between water and benzene. Thus one might estimate a value on the order of -20 e.u. per mole for the entropy change associated with the addition process, and approximately zero for the displacement process.

The entropy values for the truncated data sets in which water is the ligand (Table II) present an example of this behavior. Nd, Gd, and Ho clearly show near-zero entropies for attachment of the first water molecule, and entropies of about -11 e.u. for the second and third ligands. This suggests that the first complex is formed by substitution and the second and third by addition. La and Lu are less clear-cut, but in these cases, the second and third complexes exhibit more negative entropies than the first complex. Generally in this table for successive complexes with a given metal and for the same complex with different metals, one notes that the most negative ΔH is accompanied by the most negative ΔS . This observation is consistent with the above interpretation, in that the addition process should be more exothermic than the substitution process because in addition, there is no bond-breaking to compensate for the bond-making. Addition should also involve a larger negative entropy change because there is no molecule of solvent freed to compensate for the molecule of ligand which is bound. This explanation does not account for all details of the results set forth in Table II. Such results as the value of -39.9 e.u. for ΔS_3 for Lu may be attributable to additional processes such as an alteration in the degree of ion-pairing or reordering of the solvent sheath outside the first

coordination sphere of the metal ion.

The results for higher water concentrations shown in Table III are somewhat irregular. The ΔS_n values range from +129.8 e.u. to -154.6 e.u. These strange results may be indicative of the formation of water structure in the vicinity of the metal ions. However, they may equally be evidence for the presence of a relative minimum (or "false pit" in Sillen's terminology) in the U-surface. If these results do represent an actual process, then future studies in the area of solution structure may suggest a model which adequately explains them.

The truncated DMSO results summarized in Table V are also somewhat irregular. In this case, the difficulty arises because the first complex is so stable. Since K_1 is too large to measure accurately, the K_1 values are unreliable. This affects the entropy values, since free energy, enthalpy, and entropy, are related as shown in Equation 2. The values calculated by the direct search program for ΔH_1 agree well with those obtained graphically (using the method described earlier in the chapter). This reflects the fact that ΔH is not sensitive to K so long as K is large enough to consider the reaction to be quantitative. Although the ΔS_1 values cannot be considered very accurate in view of the above difficulties, one notes qualitatively that they average about +15 e.u. per mole. This may correspond to displacement of more than one solvent molecule by a single ligand. Here again the most positive or least negative, entropy (Gd) is associated with the least negative enthalpy.

In the case of the calculations for the higher DMSO concentrations (Table VI), the value of ΔS_9 becomes less negative as one precedes from La to Nd to Gd. This suggests the process changes from predominantly

previous description of decreasing site availability with decreasing ionic radius. As the ion becomes smaller, it gets harder and harder for a ligand to squeeze in between the solvent molecules and the ligand must more and more force out a solvent molecule (or molecules) in order to find room. ΔH_9 becomes less exothermic, which could seem contrary to the expected behavior accompanying a decrease in ionic radius, until one recognizes that the observed enthalpy change is the difference between the enthalpy connected with binding a ligand to the metal and that connected with binding a solvent molecule. Both enthalpies can become more exothermic or less, depending on the relative rates of change.

All in all, it seems that the observed coordination behavior of rare earth ions with water and DMSO can be explained in terms of two effects of the decrease in ionic radius: an increasing probability of site occupation accompanied by a decrease in total site availability. Apparent deviations from this model are due to the fact that the process under study involves competition between ligand and solvent molecules, and that the ligand may either insert itself between the coordinating solvent molecules or may be forced to eject one or more of them to secure access to a coordination site.

A somewhat similar explanation can be advanced for the trends that are observed in forming the four successive complexes between the lanthanide ions and ethylenediamine in acetonitrile (19). The first two complexes are formed with increasingly exothermic values for the process as one crosses the period. This is because the complexes are quite robust, relative to the acetonitrile interaction, so that the solvent molecules cannot crowd the ligand effectively. The third complex shows a minimum late in the series, because on the smallest ions the

ethylenediamine molecules are beginning to crowd each other. The fourth set of enthalpy changes shows a minimum earlier in the series because the crowding is more severe.

Johnston (21) has postulated that the maxima observed in the molar conductance values for the lanthanide halides in anhydrous alcohols are due to the fact that the solvent is preferred over the halide anions in these systems and that the solvation number is a maximum in the middle of the series, thus emphasizing the preference for solvent as a ligand. The process proposed in this study explains Johnston's results, without recourse to interactions involving the 4f electrons of the metal ions. (Johnston notes that the maximum corresponds to the greatest number of unpaired 4f electrons.)

Merbach, Pitteloud, and Jaccard (20) have reported that the solubility of the lanthanide chlorides increases across the series in both ethanol and methanol but exhibits a maximum at Dy when the solvent is 2-propanol. This behavior could be explained by noting that both methanol and ethanol are small compared to 2-propanol and should show a much smaller steric effect.

One should note that the trends which have been explained so far are not the most common trends in lanthanide coordination chemistry. Maxima are observed far more often than minima in studies of the enthalpy changes associated with rare earth complexation. More complicated behavior may well be attributed to the factors which have been mentioned previously: reordering of the solvent sheath and change in the coordination number of multidentate ligands.

CHAPTER VI

SUMMARY AND SUGGESTIONS FOR FUTURE WORK

Titration calorimetry has been used to study the interactions between the perchlorate salts of La(III), Nd(III), Gd(III), Ho(III), and Lu(III) in anhydrous acetonitrile and the ligands water and dimethyl sulfoxide. A computer program has been written to calculate the values of the stepwise enthalpies of complexation and the logarithms of the stability constants for the successive complexes. The program minimizes the error squared sum for the assumed model by a direct search method. The program is designed to accept models which involve cases where one or more ligand molecules are already attached to the central metal ion, as well as the case where the ion is initially in its uncomplexed form.

Two factors which depend on the ionic radius are regarded as responsible for the maximum in the apparent coordination number of the DMSO complexes which is observed at Gd. Increasing Coulombic attraction increases the probability of coordination site occupation as the ionic radius decreases. However, decreasing ion size also reduces the number of sites available. The coordination number is determined by a combination of these effects. Similar explanations might fit certain literature cases.

The enthalpy and entropy changes associated with the formation of the lanthanide complexes with water and DMSO indicate that ligands may bind to the metal ions both by substitution (by displacing solvent

molecules) and by addition (by squeezing into the coordination sphere between them). The entropy change associated with substitution is nearly zero, while the addition involves a decrease in entropy. The enthalpy change is somewhat smaller for the substitution than for the addition processes.

Further experimental work should be done with other small monodentate ligands in nonaqueous solvents to see if similar trends are the general rule rather than exceptions for this type of system. Both calorimetric and conductivity data could prove of value in this area.

Theoretical effort should be directed toward developing a mathematical formalism which describes quantitatively the coulombic and steric effects which were invoked to explain the results of this study. It would be quite valuable to have available a model which accurately predicts the behavior of rare earth complexes with a wide variety of ligands in a range of solvents.

A SELECTED BIBLIOGRAPHY

- (1) Moeller, T., et al., Chem. Rev., 65, 1 (1965).
- (2) Ashcroft, S. J. and C. T. Mortimer, "Thermochemistry of Transition Metal Complexes", Academic Press, London, 1870.
- (3) Hinckley, C. C., J. Amer. Chem. Soc., 91, 5160 (1969).
- (4) Wheelwright, E. J., F. H. Spedding, and G. Schwarzenbach, J. Amer. Chem. Soc., 75, 4196 (1953).
- (5) Harder, R. and S. Chaberek, J. Inorg. Nucl. Chem., 11, 197 (1959).
- (6) Moeller, T. and R. Ferrus, J. Inorg. Nucl. Chem., 20, 261 (1961).
- (7) Moeller, T. and L. C. Thompson, J. Inorg. Nucl. Chem., 24, 499 (1962).
- (8) Moeller, T. and T. M. Hseu, J. Inorg. Nucl. Chem., 24, 1635 (1962).
- (9) Hoard, J. L., B. Lee, and M. D. Lind, J. Amer. Chem. Soc., 87, 1612 (1965).
- (10) Lind, M. D., B. Lee, and J. L. Hoard, J. Amer. Chem. Soc., 87, 1611 (1965).
- (11) Yatsimirskii, K. B. and N. A. Kostromina, Russ. J. Inorg. Chem., 9, 971 (1964).
- (12) Edelin De La Praudiere, P. L. and L. A. K. Staveley, J. Inorg. Nucl. Chem., 26, 1713 (1964).
- (13) Padova, J., J. Phys. Chem., 71, 2347 (1967).
- (14) Tereshin, G. S., Russ. J. Inorg. Chem., 12, 1266 (1967).
- (15) Staveley, L. A. K., D. R. Markham, and M. R. Jones, Nature, 211, 1172 (1966).
- (16) Staveley, L. A. K., D. R. Markham, and M. R. Jones, J. Inorg. Nucl. Chem., 30, 231 (1968).
- (17) Morss, L. R., J. Phys. Chem., 75, 392 (1969).
- (18) Karraker, D. G., J. Chem. Ed., 47, 424 (1970).

- (19) Forsberg, J. H. and T. Moeller, *Inorg. Chem.*, 8, 889 (1968).
- (20) Johnston, D. O. and J. B. Harrell, *J. Chem. Eng. Data*, 11, 251 (1966).
- (21) Johnston, D. O., J. R. Boone, and R. F. Kimberlin, *J. Inorg. Nucl. Chem.*, 32, 1501 (1970).
- (22) Merbach, A., M. M. Pitteloud, and P. Jaccard, *Helv. Chim. Acta.*, 55, 44 (1972).
- (23) Wallace, G. F., Ph.D. Dissertation, Oklahoma State University, Stillwater, Oklahoma, 1972.
- (24) Christensen, J. J., et al., *J. Phys. Chem.*, 70, 2003 (1966).
- (25) Beck, M. T., "Chemistry of Complex Equilibria", Van Nostrand Reinhold, London, 1970.
- (26) Wall, F. T., "Chemical Thermodynamics", W. F. Freeman and Co., San Francisco, 1965.
- (27) Izatt, R. M., et al., *J. Phys. Chem.*, 72, 1208 (1968).
- (28) Bjerrum, J. and C. K. Jorgensen, *Acta. Chem. Scand.*, 1, 955 (1954).
- (29) Sillen, L. G., *Acta. Chem. Scand.*, 18, 1085 (1964).
- (30) Davidson, W. C., "Variable Metric Method for Minimization", ANL-5990, Rev. 2, Argonne National Laboratory, Argonne, Illinois.
- (31) Hooke, R. and T. A. Jeeves, *J. Assn. Comp. Mach.*, 8, 212 (1961).
- (32) Paoletti, P., A. Vacca, and D. Arenare, *J. Phys. Chem.*, 70, 193 (1966).
- (33) McCracken, D. M. and W. S. Dorn, "Numerical Methods and Fortran Programming", John Wiley and Sons, Inc., New York, 1964.
- (34) Fielder, G. D., M.S. Thesis, Oklahoma State University, Stillwater, Oklahoma, 1965.
- (35) Arthur, P., W. M. Haynes, and L. P. Varga, *Anal. Chem.*, 38, 1630 (1966).
- (36) Harris, P. C. and T. E. Moore, *Inorg. Chem.*, 7, 656 (1968).
- (37) Weast, R. C., Ed., "Handbook of Chemistry and Physics", The Chemical Rubber Co., Cleveland, Ohio, 1969.
- (38) Fischer, K., *Agnew. Chem.*, 48, 394 (1935).

- (39) Lingane, J. J., "Electroanalytical Chemistry", 2nd Ed., Interscience Publishers, New York, 1958.
- (40) Lane, W. J. and J. S. Fritz, U.S. Atomic Energy Commission ISC-945 (1957).
- (41) Smith, E. B., C. S. Barnes, and P. W. Carr, Anal. Chem., 44, 1663 (1972).
- (42) Hale, J. D., et al., J. Phys. Chem., 67, 2605 (1963).
- (43) IBM Manual GH20-0205-4, System/360 Scientific Subroutine Package, Version III (1970).
- (44) McCalla, T. R., "Introduction to Numerical Methods and FORTRAN Programming", John Wiley and Sons, Inc., New York, 1967.
- (45) Nagano, K. and D. E. Metzler, J. Amer. Chem. Soc., 89, 2891 (1967).
- (46) Christensen, J. J. and R. M. Izatt, "Physical Methods in Advanced Inorganic Chemistry", H. A. O. Hill and P. Day, Eds., Interscience Publishers, New York, N. Y., Chapter 11, 1968.
- (47) Powell, R. E., J. Phys. Chem., 58, 528 (1954).

APPENDIX A

COMPUTER PROGRAM AND EXPERIMENTAL DATA

```

C PROGRAM TO CALCULATE ENTHALPIES FROM BETAS AND CSF
C
C INITIALIZATION
EXTERNAL FFCT
DOUBLE PRECISION BETA,HSTP
COMMON ALP(317,10)
COMMON CM(8),CL(57,8),DTH(57,8),VL(8),NM
COMMON/TAG/IC(9)
DIMENSION BETA(9),HSTP(9),DEL(9),SIGH(9),USA(18),USB(18),SK(18)
104 FORMAT(6F10.0)
1C5 FORMAT(F10.6)
106 FORMAT(9I2)
204 FORMAT(1H0,'BETAS ',6(1PE15.4))
2C8 FORMAT(1X,'BN VALUES ',11X,6(1PE15.4))
205 FORMAT(1H0,'STEPWISE ENTHALPIES ',6F10.2)
206 FORMAT(1X,'AND THEIR STD DEVS ',5F10.2)
2C7 FORMAT(1X,'U AND EDF (U/DF) ',2X,E14.6,2X,F10.4)
209 FORMAT(1X,I2,5(5X,1PE15.4))
210 FORMAT(1H0,'UG= ',1PE15.4,3X,'EDF= ',1PE15.4,/,
21X,' N ',12X, ' LOG BETA',13X,
1'STC DEV',3X,'STEPWISE ENTHALPY',13X,'STD DEV',
44X,
3'STEPWISE ENTRDPY')
601 FORMAT(4I2)
6C2 FORMAT(1H1,4I2)
6J3 FORMAT(3F10.6)
444 FORMAT(1X,'DEC= ',F10.6)
C
C INITIAL DATA INPUT
CALL FILUP
READ(5,601)N,NNZ,NHV,KMAX
WRITE(6,602)N,NNZ,NHV,KMAX
NX=NHV
DD441=1,N
44 DEL(I)=0.0
READ(5,104)(BETA(I),I=1,N)
WRITE(6,204)(BETA(I),I=1,N)
READ(5,106)(IC(I),I=1,N)
IEDO=1
C
C FIND INITIAL U
CALL ACE(NX,NY,N,IEDO,CZ,BETA,HSTP,SIGH,UO,EDF)
IEDO=0
IX=65539
DO2 K=1,KMAX
READ(5,105)DEC
WRITE(6,444)DEC
DD11=1,N
1 IF(IC(I).GT.-3)DEL(I)=DEC
C
C CHOOSE A BETA TO VARY
10 ICD=0
5 IF(ICD.GE.NNZ)GO TO 7
3 CALL RANDU(IX,IY,XN)
IX=IY
IR=XN*N+1
IF(IC(IR).NE.0)GO TO 3
ICD=ICD+1
C
C VARY UP

```

```

BETA(IR)=BETA(IR)+DEL(IR)
CALL ACE(NX,NY,N,IEDO,CZ,BETA,HSTP,SIGH,UN,EDF)
WRITE(6,303)K,UN,(BETA(I),I=1,N)
303 FORMAT(1X,I2,5(3X,E14.6),/,5(3X,E14.6))
IF(LN.GE.UO)GO TO 4
UO=UN
IC(IR)=1
GO TO 5
4 USA(IR)=UN
C
C VARY DOWN
BETA(IR)=BETA(IR)-2.0*DEL(IR)
CALL ACE(NX,NY,N,IEDO,CZ,BETA,HSTP,SIGH,UN,EDF)
IF(LN.GE.UO)GO TO 6
IC(IR)=1
DEL(IR)=-DEL(IR)
UO=UN
GO TO 5
6 USB(IR)=UN
IC(IR)=-1
C
C RETAIN ORIGINAL BETA IF VARIATION DOES NOT LOWER J
BETA(IR)=BETA(IR)+DEL(IR)
GO TO 5
C
C TEST FOR CONVERGANCE
7 DD91=1,N
IF(IC(I).GT.0)GO TO 8
IF(IC(I).EQ.0)GO TO 99
9 CONTINUE
GO TO 21
8 DO 11 I=1,N
11 IF(IC(I).GT.-3)IC(I)=0
GO TO 10
21 DD22I=1,N
22 IF(IC(I).GT.-3)IC(I)=0
2 CONTINUE
C
C VARY DELTA H AND OBSERVE U
DO 16 I=1,N
NI=N+I
HSX=HSTP(I)
HSTP(I)=HSTP(I)+DEC*HSX
CALL ACEX(NX,NY,N,BETA,HSTP,UX)
USA(NI)=UX
HSTP(I)=HSTP(I)-2*DEC*HSX
CALL ACEX(NX,NY,N,BETA,HSTP,UX)
USB(NI)=UX
HSTP(I)=HSX
16 SK(NI)=DEC*HSX*(0.5*(1/(USA(NI)-UO)+1/(USB(NI)-UO))*EDF)**0.5
12 IEDC=1
CALL ACE(NX,NY,N,IEDO,CZ,BETA,HSTP,SIGH,UO,EDF)
DD13KTT=1,N
IF(IC(KTT).LE.-3)GO TO 13
SK(KTT)=DEL(KTT)*(0.5*(1/(USA(KTT)-UO)+1/(USB(KTT)-UO))*EDF)**0.5
13 CONTINUE
DIMENSION SSTP(9)
C
C CALCULATE ENTROPY CHANGE
DO 15 I=1,N

```



```

IF(IC(I).EQ.-7)GO TO 15
SSTP(I)=1.987*2.303*BET A(I)+HSTP(I)/298
15 CONTINUE
C
C PRINT RESULTS
WRITE(6,210)UO,EOF
DO14 I=1,N
NI=N+I
IF(IC(I).EQ.-7)GO TO 14
WRITE(6,209)I,BET A(I),SK(I),HSTP(I),SK(NI),SSTP(I)
14 CONTINUE
99 CONTINUE
STOP
END

SUBROUTINE FILUP
C READS IN RAW DATA FOR MAIN
C *****THE WRITE STATEMENTS INCLUDED AS COMMENT CARDS MAY BE USED
C *****INSTEAD OF THOSE CURRENTLY ACTIVE, OR IN ADDITION TO THEM.
C *****FORMATS FOR BOTH ARE INCLUDED.
COMMON ALP(317,10)
COMMON CMA(8),CL(57,8),DTH(57,8),NL(8),I
PROGRAM TO CALCULATE C.S.F. FROM RAW DATA
101 FORMAT(5A4,3F10.6,I2)
102 FORMAT(5F10.6,I2,A4)
103 FORMAT(2F10.6)
104 FORMAT(2F10.6)
201 FORMAT(1H1,5A4,/,1X,' LIGAND DENSITY, MOL WT, HEAT OF DIL, VD,
IRUNS ',3(2X,F14.6),2X,I2)
202 FORMAT(1H0,'METAL CON ',F10.6,3X,A4,/,1X,'SAMPLE VOL, CFI, CPF,
1ML ADDED, NO PTS, INIT Q AND CL',/,1X,4(2X,F14.6),2X,I2,2(2X,F14.6
2)I)
203 FORMAT(1H0,1X,'CAL/MOL M MOLARITY LIG')
204 FORMAT(1X,F10.2,5X,F10.6,10X,F10.6,2X,F10.6)
READ(5,500)BX,BY,BZ,BA,BB
500 FORMAT(5A4)
READ(5,101)AA,AB,AC,AD,AE,RHO,RMW,QDIL,I
C
WRITE(6,201)AA,AB,AC,AD,AE,RHO,RMW,QDIL,I
DO1K=1,I
READ(5,102)CM,V,CPI,CPF,TML,IA,AF
NL(K)=IA
CMA(K)=CM
READ(5,103)CLI,QI
CSF=QI
RMH=CM*V*0.001
C
WRITE(6,202)CM,AF,V,CPI,CPF,TML,IA,QI,CLI
C
WRITE(6,203)
601 FORMAT(1H0,1X,5A4,/,1X,'CM= ',F7.5,/,1X,'LIG CON',3X,'CAL/MOLE')
DCP=(CPF-CPI)/TML
VD=0.0
DO2KA=1,IA
READ(5,104)VI,CH
CLC=((VI*RHO)/RMW)/(V/1000.)*CLI
CL(KA,K)=CLC
VX=VI-VD
VO=VI
CQ=((-1*CH)*(CPI+DCP*VI)-(QDIL*VX))/RMH

```

```

CSF=CSF+CQ
DTH(KA,K)=CSF
C
WRITE(6,204)CSF,CLC,V1,CH
WRITE(6,602)CLC,CSF
602 FORMAT(1X,F7.4,3X,F8.0)
2 CONTINUE
1 CONTINUE
RETURN
END

SUBROUTINE ACE(NX,NY,N,IEDO,CZ,BETA,HSTP,SIGH,J,EOF)
C
C CALCULATES ENTHALPIES AND U FROM BETAS AND CSF DATA
C
C INITIALIZE
COMMON ALP(317,10)
COMMON CM(8),CL(57,8),DTH(57,8),NL(8),NM
COMMON/TAG/IC(9)
DOUBLE PRECISION DAVE,BTX,WGT
DIMENSION ALPS(10),DAVE(1),BTX(9)
EXTERNAL FFCT
DOUBLE PRECISION BETA,AX,BX,HS,HSTP
201 FORMAT(1X,'ITERI= ',I2)
205 FORMAT(1X,'ICON,CMX,CLX ',
1 I2,2(2X,F10.6))
DOUBLE PRECISION WORK,DATI,P,A
DIMENSION BETA(9),HSTP(9),SIGH(9),WORK(55),DATI(1),P(10),
1A(55),HS(9),AX(55),BX(81),L(9),M(9)
ANZ=NX
DO59IX=1,55
WORK(IX)=0.0
A(IX)=0.0
99 AX(IX)=0.0
DO98IXA=1,9
BTX(IXA)=0.0
HS(IXA)=0.0
L(IXA)=0.0
98 M(IXA)=0.0
DO97IXB=1,81
BX(IXB)=0.0
DO56IXC=1,10
P(IXC)=0.0
NSC=NM*2
DO33IS4=1,N
IF(IC(I54).EQ.-7)GO TO 33
C
C CONVERT LOG BETA TO BETA
BTX(I54)=10.0**BETA(I54)
23 CONTINUE
NF=NNZ+1
IP=0
DO4CI=1,NM
CMX=CM(I)
CLX=CL(I,I)
CALL CON(CMX,CLX,FM,FL,BTX,ICON,N)
JN=0
C
C CALCULATE ALPHAS FOR 1-ST POINT OF EACH RUN
DO4IJ=1,N
IF(BTX(J).LE.0.0)GO TO 41
JN=JN+1

```

```

ALPS(JN)=BTX(J)*FM*FL**J/CM(I)
41 CONTINUE
ALP(NF)=DTH(1,I)
NLX=NL(I)
DC4OK=2,NLX
IP=IP+1
CLX=CL(K,I)
CALL CON(CMX,CLX,F4,FL,BTX,ICDN,N)
JN=C
C
C CALCULATE ALPHAS FOR N-TH POINT AND SUBTRACT
C ALPHAS FOR 1-ST POINT
DD4ZJ=1,N
IF(BTX(J).LE.0.0)GO TO 42
JN=JN+1
ALP(IP,JN)= BTX(J)*FM*FL**J/CM(I)-ALPS(JN)
42 CONTINUE
40 ALP(IP,NF)=DTH(K,I)-ALPS(NF)
NP=IP
FPS=1.0E-15
IM=1
IL=1
C
C OBTAIN THE COEFFICIENT MATRIX AND ITS INVERSE; OBTAIN DELTA H'S
CALL CAPL(FFCT,NP,NNZ,P,WORK,DAVE,IER1)
IF(ITER1.NE.0)WRITE(6,201)IER1
IZ= ((NNZ+1)*(NNZ+2))/2-(NNZ+1)
DO2 IZA=1,IZ
2 AX(IZA)=WORK(IZA)
CALL DXNV(AX,BX,NNZ)
I11=0
DO5 IZB=1,NNZ
5 HS(IZB)=WORK(IZ+IZB)
CALL DPRD(BX,HS,HSTP,NNZ,NNZ,0,0,1)
C
C CALCULATE U AND PCT DEV
U=0.0
YSUM=0.0
PCTD=0.0
IM=1
IL=1
DO3 KX=1,NP
CALL FFCT(KX,NP,NNZ,P,DAVE,WGT,IER)
SU=0.0
DO6 KXX=1,NNZ
6 SU=SU+P(KXX)*HSTP(KXX)
PXT=P(NNZ+1)
PCTD=PCTD+(ABS(SU-PXT)/PXT)*100.0
IF(IEDO.EQ.1)WRITE(6,5005)SU,P(NNZ+1)
5005 FORMAT(1X,'DELTA CSF CALC= ',F10.1,'
YSUM=YSUM+P(NNZ+1)
3 U=U+(SU-P(NNZ+1))**2
EDF=U/(NP-2*NNZ)
PCTD=PCTD/NP
IF(IEDO.EQ.1)WRITE(6,5006)PCTD
5006 FORMAT(1X,'PCT AVE DEV ',F10.3)
11 RETURN
END

```

EXP= ',F10.1)

```

SUBROUTINE CONICMX,CLX,RM,RLA,BETA,ICON,N)
C USFS NEWTON-RAPHSON ITERATIVE METHOD TO CALCULATE
C FREE LIGAND AND FREE METAL CONCENTRATIONS
DIMENSION BETA(9)
DOUBLE PRECISION BETA
ICCN=1
9 B9=BETA(9)
8 B8=BETA(8)
17 B7=BETA(7)
6 B6=BETA(6)
5 B5=BETA(5)
4 B4=BETA(4)
3 B3=BETA(3)
2 B2=BETA(2)
1 B1=BETA(1)
RLA=CLX/(CMX*100.0)
DO7 K=1,300
RM=CMX/(1.+B1*RLA+B2*RLA**2+B3*RLA**3+B4*RLA**4+B5*RLA**5
1+B6*RLA**6+B7*RLA**7+B8*RLA**8+B9*RLA**9)
G=RLA+B1*RLA*RM+2.*B2*RM*RLA**2+3.*B3*RM*RLA**3+4.*B4*RM*RLA**4
1+5.*B5*RM*RLA**5+6.*B6*RM*RLA**6-CLX
2+7.*B7*RM*RLA**7+8.*B8*RM*RLA**8+9.*B9*RM*RLA**9
DGL=B1*RM+4.*B2*RM*RLA+9.*B3*RM*RLA**2+16.*B4*RM*RLA**3
1+25.*B5*RM*RLA**4+36.*B6*RM*RLA**5+1
2+49.*B7*RM*RLA**6+64.*B8*RM*RLA**7+81.*RM*RLA**8
RLB=RLA-G/DGL
RX=ABS(RLA-RLB)
IF(RX.LE.(0.001*RLA))GO TO 1000
IF(K.GT.30)RLB=(RLA+RLB)/2
RLB=(RLA+RLB)/2
IF((RLB**2).GE.100000.0)GO TO 1001
7 RLA=RLB
ICON=2
1000 RETURN
1001 ICON=3
RETURN
END
SUBROUTINE ACEX(NX,NY,N,BETA,HSTP,UX)
C CALCULATE U FROM SUPPLIED VALUES OF BETA'S AND HSTP'S
COMMON ALP(317,10)
COMMON CM(8),CL(57,8),DTH(57,8),NL(8),NM
COMMON/TAG/IC(9)
EXTERNAL FFCT
DOUBLE PRECISION BETA,HSTP,P,DAVE,WGT,BTX
DIMENSION BTX(9),BETA(9),ALPS(10),P(10),DAVE(1),HSTP(9)
DO 37 I=1,9
37 BTX(I)=0.0
DO33 I54=1,N
IF(IC(I54).EQ.-7)GO TO 33
BTX(I54)=10.0**BETA(I54)
33 CONTINUE
NNZ=NX
NF=NNZ+1
IP=0
DO401=1,NM
CMX=CM(I)
CLX=CL(I,I)

```

```

CALL CON(CMX,CLX,FM,FL,BTX,ICON,N)
JN=0
DO41 J=1,N
IF(BTX(J).LE.0.0)GO TO 41
JN=JN+1
ALPS(JN)=BTX(J)*FM*FL**J/CM(I)
41 CONTINUE
ALPS(NF)=DTH(1,I)
NLX=NL(I)
DO40K=2,NLX
IP=IP+1
CLX=CL(K,I)
CALL CON(CMX,CLX,FM,FL,BTX,ICON,N)
JN=0
DO42J=1,N
IF(BTX(J).LE.0.0)GO TO 42
JN=JN+1
ALP(IP,JN)= BTX(J)*FM*FL**J/CM(I)-ALPS(JN)
42 CONTINUE
40 ALP(IP,NF)=DTH(K,I)-ALPS(NF)
NP=IP
U=0.0
DO3KX=1,NP
CALL FFCT(KX,NP,NNZ,P,DAVE,WGT,IER)
SU=0.0
DO6KXX=1,NNZ
6 SU=SU+P(KXX)*HSTP(KXX)
3 U=U+(SU-P(NNZ+1))**2
UX=L
RETURN
END

```

```

SUBROUTINE DPRD(A,B,R,N,M,MSA,MSB,L)
C MULTIPLIES TWO MATRICES TOGETHER AND RETURNS THEIR PRODUCT
DIMENSION A(1),B(1),R(1)
DOUBLE PRECISION A,B,R
MS=MSA*10+MSB
IF(MS-22)30,10,30
10 DO2CI=1,N
20 R(I)=A(I)*B(I)
RETURN
30 IR=1
DO9OK=1,L
DO9OJ=1,N
R(IR)=0
DOBOI=1,M
IF(MS)40,60,40
40 CALL LOC(J,I,IA,N,M,MSA)
CALL LOC(I,K,IB,M,L,MSB)
IF(IA) 50,80,50
50 IF(IB) 70,80,70
60 IA=N*(I-1)+J
IB=M*(K-1)+I
70 R(IR)=R(IR)+A(IA)*B(IB)
80 CONTINUE
90 IR=IR+1
RETURN
END

```

```

SUBROUTINE DXNVIC(B,NX)
C USES HOTELLING'S METHOD TO IMPROVE AN APPROXIMATE INVERSE OF A MATRIX
DOUBLE PRECISION DABS
N=N*
DOUBLE PRECISION A,B,AMAX,ATMP,BTMP,DEL,DIV,AMULT,DI,E,R
EPS=1.0E-12
DIMENSION A(9,9),B(9,9),DI(9,9),E(9,9),R(9,9),L(1),M(1)
DO6I=1,N
CO5J=1,N
IF(I-J)4,3,4
3 B(I,J)=1.0D+00
DI(I,J)=1.0D+00
E(I,J)=0.0
R(I,J)=0.0
GO TO 5
4 B(I,J)=0.0
DI(I,J)=0.0
E(I,J)=0.0
R(I,J)=0.0
5 CONTINUE
6 CONTINUE
DOUBLE PRECISION C
DIMENSION C(28)
CALL DSTR(C,A,N,1,J)
CALL DSINVIC,NX,EPS,IER)
IF(IER.NE.0)WRITE(6,104)IER
CALL DSTRIC(B,N,1,0)
104 FORMAT(1X,'IER FROM DSINV',I3)
CALL DPRD(A,B,R,N,N,0,0,N)
CALL DRRAY(1,N,N,9,9,R,R)
DO50I=1,N
DO50J=1,N
50 E(I,J)=DI(I,J)-R(I,J)
DO52I=1,N
SIG=0.0
DO51J=1,N
51 SIG=SIG+DABS(E(I,J))
IF(SIG.GE.1.0)GOTO94
52 CONTINUE
DO95K=1,20
DO53I=1,N
DO53J=1,N
53 E(I,J)=DI(I,J)+E(I,J)
CALL DRRAY(2,N,N,9,9,E,E)
CALL DRRAY(2,N,N,9,9,R,R)
CALL DPRD(B,E,R,N,N,0,0,N)
CALL DRRAY(1,N,N,9,9,R,R)
CALL DRRAY(1,N,N,9,9,B,B)
DO54I=1,N
CO54J=1,N
54 B(I,J)=R(I,J)
CALL DRRAY(2,N,N,9,9,B,B)
CALL DPRD(A,B,R,N,N,0,0,N)
CALL DRRAY(1,N,N,9,9,R,R)
DO55I=1,N
CO55J=1,N
55 E(I,J)=DI(I,J)-R(I,J)
DO56I=1,N
SIG=0.0
DO57J=1,N

```

```

57 SIG=SIG+DABS(E(I,J))
  IF(SIG.GE.(.00001))GO TO 95
56 CONTINUE
  GO TO96
95 CONTINUE
  WRITE(6,101)
101 FORMAT(1X,'HOTELLING DID NOT REACH LIMIT')
96 CONTINUE
  RETURN
54 WRITE(6,102)
102 FORMAT(1X,'HOTELLING CANNOT BE USED')
  RETURN
53 WRITE(6,103)
103 FORMAT(1X,'MATRIX IS SINGULAR')
  RETURN
  END

```

```

SUBROUTINE USTR(A,R,N,MSA,MSR)
C CONVERTS MATRICES FROM ONE STORAGE TYPE TO ANOTHER
  DIMENSION A(1),R(1)
  DOUBLE PRECISION A,R
  DO2J=1,N
  DO2CJ=1,N
  IF(MSR)5,10,5
  5 IF(I-J)10,10,20
  10 CALL LOC(I,J,IR,N,N,MSR)
  IF(IR)20,20,15
  15 R(IR)=0.0
  CALL LOC(I,J,IA,N,N,MSA)
  IF(IA)20,20,18
  18 R(IR)=A(IA)
  20 CONTINUE
  RETURN
  END

```

```

SUBROUTINE DRRAY(MODE,I,J,N,M,S,D)
C CONVERTS MATRICES BETWEEN VECTOR MODE AND DOUBLE SUBSCRIPT MODE
  DIMENSION S(1),D(1)
  DOUBLE PRECISION S,D
  NI=N-1
  IF(MODE-1)100,100,120
100 IJ=I+J+1
  NM=N+J+1
  DO110K=1,J
  NM=NM-NI
  DO110L=1,I
  IJ=IJ-1
  NM=NM-1
110 D(NM)=S(IJ)
  GO TO 140
120 IJ=0
  NM=0
  DO130K=1,J
  DO125L=1,I
  IJ=IJ+1
  NM=NM+1
125 S(IJ)=D(NM)
130 NM=NM+NI
140 RETURN
  END

```

```

SUBROUTINE FFCT(I,NP,N,P,DATI,WGT,IER)
C LOOKS UP ALPHAS FROM COMMON
  DOUBLE PRECISION P,DATI,WGT
  DIMENSION P(10),DATI(1)
  COMMON ALP(317,10)
  COMMON CM(8),CL(57,8),DTH(57,8),NL(8),NM
  WGT=1.00+00
  DOIJ=1,N
  1 P(IJ)=ALP(I,J)
  P(N+1)=ALP(I,N+1)
  3 RETURN
  END

```

LA VS WATER
CM= 0.01545

LIG CON	CAL/MOLE
0.0151	-1700.
0.0194	-2854.
0.0237	-3910.
0.0324	-5882.
0.0410	-7769.
0.0496	-9467.
0.0582	-11008.
0.0668	-12431.
0.0754	-13714.
0.0841	-14880.
0.0927	-15957.

LA VS WATER
CM= 0.01545

LIG CON	CAL/MOLE
0.0108	-744.
0.0151	-1881.
0.0237	-4199.
0.0323	-6294.
0.0409	-8194.
0.0495	-9964.
0.0581	-11561.
0.0753	-14311.
0.0925	-16563.

LA VS WATER
CM= 0.03023

LIG CON	CAL/MOLE
0.0162	-1273.
0.0248	-2643.
0.0334	-4082.
0.0420	-5484.
0.0506	-6795.
0.0592	-8073.
0.0678	-9306.
0.0764	-10461.
0.0850	-11591.
0.0936	-12615.
0.1108	-14588.
0.1280	-16345.
0.1452	-17919.
0.1624	-19326.
0.1796	-20592.
0.1968	-21732.

LA VS WATER
CM= 0.03023

LIG CON	CAL/MOLE
0.0162	-1342.
0.0248	-2723.
0.0334	-4078.
0.0421	-5467.
0.0507	-6695.
0.0593	-7903.
0.0679	-9095.
0.0765	-10226.
0.0851	-11265.
0.0938	-12284.
0.1024	-13259.
0.1110	-14169.
0.1196	-15045.
0.1282	-15856.
0.1368	-16631.
0.1455	-17371.
0.1541	-18069.
0.1627	-18725.
0.1713	-19347.
0.1799	-19938.
0.1885	-20504.
0.1972	-21039.

LA VS WATER
CM= 0.06309

LIG CON	CAL/MOLE
0.0493	-1345.
0.0665	-2876.
0.0838	-4316.
0.1010	-5768.
0.1182	-7151.
0.1355	-8490.
0.1527	-9817.
0.1699	-11098.
0.1872	-12292.
0.2044	-13450.
0.2475	-16166.
0.2906	-18577.
0.3337	-20675.
0.3768	-22505.
0.4625	-25502.

LA VS WATER
CM= 0.04635

LIG CON	CAL/MOLE
0.0367	-1835.
0.0539	-3807.
0.0711	-5721.
0.0883	-7474.
0.1055	-9218.
0.1227	-10858.
0.1571	-13932.
0.1916	-16622.
0.2346	-19478.
0.2776	-21865.
0.3636	-25546.

LA VS WATER
CM= 0.04635

LIG CON	CAL/MOLE
0.0367	-2009.
0.0540	-3983.
0.0712	-5850.
0.0884	-7701.
0.1057	-9436.
0.1225	-11106.
0.1401	-12678.
0.1574	-14096.
0.1919	-16820.
0.2349	-19683.
0.2780	-22097.
0.3642	-25814.

LA VS WATER
CM= 0.06309

LIG CON	CAL/MOLE
0.0493	-1210.
0.0665	-2745.
0.0837	-4218.
0.1009	-5658.
0.1181	-7066.
0.1353	-8421.
0.1525	-9743.
0.1697	-11003.
0.1869	-12229.
0.2041	-13413.
0.2471	-16149.
0.2901	-18562.
0.3332	-20658.
0.3762	-22495.
0.4622	-25511.

ND VS WATER
CM= 0.01511

LIG CON	CAL/MOLE
0.0325	-1139.
0.0368	-2379.
0.0437	-4277.
0.0497	-5772.
0.0541	-6781.
0.0627	-8587.
0.0713	-10191.
0.0799	-11595.
0.0885	-12835.
0.0971	-14049.

ND VS WATER
CM= 0.01511

LIG CON	CAL/MOLE
0.0325	-1276.
0.0368	-2454.
0.0411	-3559.
0.0471	-5056.
0.0540	-6547.
0.0626	-8197.
0.0712	-9637.
0.0798	-10917.
0.0884	-12045.

ND VS WATER
CM= 0.03115

LIG CON	CAL/MOLE
0.0302	-1357.
0.0386	-2796.
0.0471	-4202.
0.0556	-5534.
0.0641	-6792.
0.0725	-7993.
0.0895	-10240.
0.1064	-12233.
0.1234	-14005.
0.1403	-15564.
0.1657	-17560.
0.1911	-19217.

ND VS WATER
CM= 0.03115

LIG CON	CAL/MOLE
0.0303	-1243.
0.0389	-2757.
0.0476	-4190.
0.0562	-5570.
0.0648	-6892.
0.0734	-8133.
0.0906	-10463.
0.1079	-12495.
0.1251	-14310.
0.1423	-15899.
0.1682	-17925.
0.1941	-19621.

ND VS WATER
CM= 0.06163

LIG CON	CAL/MOLE
0.0338	-1463.
0.0510	-3108.
0.0682	-4687.
0.0854	-6220.
0.1026	-7697.
0.1198	-9094.
0.1370	-10455.
0.1628	-12310.
0.1887	-14060.
0.2231	-16148.
0.2747	-18843.
0.3607	-22471.
0.4467	-25400.

ND VS WATER
CM= 0.06163

LIG CON	CAL/MOLE
0.0338	-1543.
0.0511	-3200.
0.0683	-4823.
0.0855	-6358.
0.1028	-7869.
0.1200	-9312.
0.1372	-10686.
0.1631	-12644.
0.1890	-14446.
0.2234	-16646.
0.2751	-19441.
0.3613	-23063.
0.4475	-25732.

ND VS WATER
CM= 0.04680

LIG CON	CAL/MOLE
0.0255	-762.
0.0345	-1821.
0.0431	-2850.
0.0517	-3874.
0.0603	-4863.
0.0689	-5828.
0.0775	-6763.
0.0861	-7693.
0.1033	-9442.
0.1205	-11097.
0.1377	-12625.
0.1545	-14039.
0.1721	-15353.
0.1894	-16567.
0.2066	-17676.
0.2236	-18693.
0.2496	-20068.
0.2754	-21276.
0.3012	-22357.

ND VS WATER
CM= 0.04680

LIG CON	CAL/MOLE
0.0255	-873.
0.0345	-1925.
0.0432	-2979.
0.0518	-4001.
0.0604	-4994.
0.0690	-5985.
0.0776	-6897.
0.0862	-7822.
0.0949	-8695.
0.1035	-9557.
0.1121	-10387.
0.1207	-11208.
0.1293	-11998.
0.1379	-12765.
0.1466	-13492.
0.1552	-14200.
0.1724	-15526.
0.1983	-17324.
0.2241	-18897.
0.2500	-20287.
0.2758	-21509.
0.3017	-22608.

GD VS WATER
CM= 0.01536

LIG CON	CAL/MOLE
0.0213	-1301.
0.0256	-2492.
0.0342	-4849.
0.0429	-6685.
0.0532	-8722.
0.0601	-9936.
0.0687	-11226.
0.0773	-12395.
0.0859	-13440.

GD VS WATER
CM= 0.01536

LIG CON	CAL/MOLE
0.0213	-1016.
0.0256	-2122.
0.0342	-4386.
0.0428	-6382.
0.0514	-8240.
0.0600	-9852.
0.0686	-11733.
0.0772	-12793.
0.0858	-13909.

GD VS WATER
CM= 0.06020

LIG CON	CAL/MOLE
0.0462	-1530.
0.0634	-3114.
0.0806	-4621.
0.0978	-6101.
0.1150	-7518.
0.1408	-9584.
0.1666	-11492.
0.2011	-13852.
0.2441	-16435.
0.2871	-18660.
0.3731	-22243.
0.4591	-24924.

GD VS WATER
CM= 0.06020

LIG CON	CAL/MOLE
0.0462	-1603.
0.0635	-3206.
0.0807	-4769.
0.0979	-6282.
0.1152	-7785.
0.1410	-9895.
0.1669	-11848.
0.2014	-14231.
0.2875	-19165.
0.3306	-21106.
0.3737	-22770.
0.4599	-25474.

GD VS WATER
CM= 0.05850

LIG CON	CAL/MOLE
0.0308	-1491.
0.0480	-3192.
0.0652	-4872.
0.0824	-6496.
0.0996	-8093.
0.1254	-10461.
0.1512	-12669.
0.1857	-15500.
0.2287	-18701.
0.2717	-21391.
0.3147	-23710.
0.3577	-25626.
0.4437	-28575.

GD VS WATER
CM= 0.05850

LIG CON	CAL/MOLE
0.0308	-1547.
0.0481	-3234.
0.0653	-4903.
0.0825	-6543.
0.0998	-8071.
0.1256	-10386.
0.1515	-12570.
0.1860	-14845.
0.2290	-17966.
0.2721	-20640.
0.3152	-22894.
0.3583	-24777.
0.4445	-27713.

HD VS WATER
CM= 0.01373

LIG CON	CAL/MOLE
0.0204	-2010.
0.0290	-4773.
0.0377	-7293.
0.0463	-9646.
0.0549	-11747.
0.0635	-13547.
0.0721	-15142.
0.0807	-16519.

HD VS WATER
CM= 0.01373

LIG CON	CAL/MOLE
0.0161	-1050.
0.0204	-2456.
0.0247	-3915.
0.0290	-5332.
0.0376	-7834.
0.0462	-10142.
0.0548	-12273.
0.0634	-14112.
0.0806	-17094.

LU VS WATER
CM= 0.02254

LIG CON	CAL/MOLE
0.0314	-1422.
0.0395	-3540.
0.0476	-5702.
0.0557	-7679.
0.0638	-9553.
0.0719	-11286.
0.0800	-13014.
0.0881	-14600.
0.0962	-16028.
0.1043	-17354.
0.1205	-19618.
0.1367	-21464.
0.1529	-22966.

LU VS WATER
CM= 0.02254

LIG CON	CAL/MOLE
0.0314	-1560.
0.0404	-3818.
0.0489	-5996.
0.0574	-8111.
0.0660	-10069.
0.0745	-11959.
0.0830	-13667.
0.0916	-15345.
0.1001	-16838.
0.1086	-18177.
0.1257	-20425.
0.1427	-22249.
0.1598	-23720.

LU VS WATER
CM= 0.01484

LIG CON	CAL/MOLE
0.0272	-1671.
0.0358	-4443.
0.0444	-7323.
0.0529	-9955.
0.0615	-12265.
0.0701	-14259.
0.0873	-17485.
0.1044	-19788.

LU VS WATER
CM= 0.01484

LIG CON	CAL/MOLE
0.0270	-1763.
0.0354	-5022.
0.0438	-7719.
0.0522	-10254.
0.0606	-12525.
0.0689	-14431.
0.0857	-17461.
0.1025	-19626.

LA VS OMSO
CM= 0.01700

LIG CON	CAL/MOLE
0.0043	-1552.
0.0085	-3075.
0.0128	-4562.
0.0170	-5984.
0.0213	-7384.
0.0256	-8763.
0.0298	-10046.
0.0341	-11323.
0.0384	-12600.
0.0426	-13834.
0.0469	-15074.
0.0511	-16293.
0.0575	-18100.
0.0639	-19908.
0.0703	-21759.
0.0767	-23610.
0.0831	-25448.
0.0895	-27190.
0.0959	-28882.
0.1023	-30458.
0.1087	-31859.
0.1172	-33543.
0.1279	-35204.
0.1385	-36427.
0.1492	-37323.
0.1705	-38516.
0.1918	-39207.
0.2131	-39650.
0.2344	-39946.
0.2557	-40141.
0.2770	-40298.
0.2983	-40427.
0.3197	-40526.

LA VS OMSO
CM= 0.01700

LIG CON	CAL/MOLE
0.0043	-1652.
0.0085	-3239.
0.0139	-5098.
0.0181	-6581.
0.0213	-7666.
0.0256	-9093.
0.0298	-10462.
0.0342	-11779.
0.0384	-13076.
0.0427	-14379.
0.0471	-15529.
0.0512	-16913.
0.0555	-18143.
0.0598	-19432.
0.0640	-20691.
0.0683	-21979.
0.0726	-23282.
0.0769	-24577.
0.0811	-25822.
0.0854	-27044.
0.0897	-28252.
0.0939	-29446.
0.0982	-30545.
0.1025	-31622.
0.1067	-32591.
0.1110	-33530.
0.1153	-34404.
0.1217	-35516.
0.1281	-36475.
0.1345	-37275.
0.1409	-37908.
0.1494	-38626.
0.1601	-39299.
0.1708	-39805.
0.1921	-40476.
0.2135	-40908.
0.2348	-41195.
0.2562	-41410.
0.2775	-41589.
0.2989	-41709.
0.3202	-41808.
0.3416	-41886.
0.3629	-41941.

LA VS DMSO
CM= 0.07258

LIG CON	CAL/MOLE
0.0107	-907.
0.0213	-1850.
0.0320	-2807.
0.0427	-3701.
0.0534	-4645.
0.0640	-5560.
0.0747	-6472.
0.0854	-7358.
0.0961	-8229.
0.1067	-9109.
0.1174	-9945.
0.1281	-10808.
0.1388	-11633.
0.1494	-12438.
0.1601	-13251.
0.1708	-14073.
0.1815	-14882.
0.1921	-15696.
0.2028	-16501.
0.2135	-17310.
0.2242	-18104.
0.2348	-18897.
0.2455	-19686.
0.2562	-20484.
0.2668	-21026.
0.2882	-21842.
0.2989	-22632.
0.3095	-23430.
0.3202	-24228.
0.3309	-25018.
0.3416	-25816.
0.3522	-26614.
0.3629	-27425.
0.3736	-28240.
0.3843	-29051.
0.3949	-29849.
0.4056	-30648.
0.4163	-31455.
0.4270	-32270.
0.4483	-33889.
0.4697	-35471.
0.4910	-37032.
0.5123	-38532.
0.5337	-39949.
0.5550	-41235.
0.5764	-42422.
0.5977	-43485.
0.6191	-44366.
0.6404	-45115.
0.6618	-45728.
0.6831	-46187.
0.7045	-46544.
0.7258	-46834.
0.7472	-47062.
0.7685	-47258.
0.7899	-47432.

LA VS DMSO
CM= 0.07258

LIG CON	CAL/MOLE
0.0213	-1894.
0.0426	-3738.
0.0639	-5592.
0.0852	-7388.
0.1066	-9118.
0.1279	-10823.
0.1492	-12479.
0.1705	-14102.
0.1918	-15683.
0.2131	-17274.
0.2344	-18850.
0.2557	-20367.
0.2770	-21919.
0.2983	-23465.
0.3197	-25020.
0.3410	-26594.
0.3623	-28170.
0.3836	-29798.
0.4049	-31394.
0.4262	-32947.
0.4475	-34519.
0.4688	-36067.
0.4901	-37581.
0.5114	-39036.
0.5328	-40423.
0.5541	-41680.
0.5754	-42851.
0.5967	-43875.
0.6180	-44761.
0.6393	-45507.
0.6606	-46114.
0.6819	-46591.
0.7032	-46972.
0.7245	-47265.
0.7459	-47505.
0.7672	-47695.
0.7885	-47865.

LA VS DMSO
CM= 0.03249

LIG CON	CAL/MOLE
0.0664	-1191.
0.0128	-2402.
0.0192	-3662.
0.0256	-4863.
0.0320	-6064.
0.0384	-7245.
0.0465	-8804.
0.0554	-10294.
0.0639	-11745.
0.0746	-13573.
0.0852	-15313.
0.0955	-16984.
0.1066	-18694.
0.1172	-20395.
0.1275	-22066.
0.1385	-23787.
0.1492	-25499.
0.1601	-27548.
0.1705	-28922.
0.1811	-30683.
0.1918	-32375.
0.2024	-34008.
0.2131	-35592.
0.2238	-37067.
0.2344	-38444.
0.2451	-39742.
0.2557	-40902.
0.2770	-42640.
0.2983	-43864.
0.3197	-44713.
0.3410	-45306.
0.3623	-45720.
0.3836	-45996.
0.4049	-46213.
0.4262	-46381.
0.4475	-46499.
0.4688	-46607.

LA VS DMSO
CM= 0.03249

LIG CON	CAL/MOLE
0.0064	-1181.
0.0128	-2382.
0.0192	-3354.
0.0256	-4495.
0.0320	-5655.
0.0384	-6975.
0.0470	-8605.
0.0555	-10225.
0.0640	-11795.
0.0747	-13576.
0.0854	-15406.
0.0961	-17216.
0.1067	-18976.
0.1174	-20776.
0.1281	-22556.
0.1388	-24335.
0.1494	-26154.
0.1601	-27992.
0.1708	-29731.
0.1815	-31549.
0.1921	-33396.
0.2028	-35233.
0.2135	-36921.
0.2242	-38560.
0.2348	-40079.
0.2455	-41460.
0.2562	-42691.
0.2775	-44600.
0.2989	-45895.
0.3202	-46795.
0.3416	-47348.
0.3629	-47762.
0.3843	-48077.
0.4056	-48314.
0.4270	-48491.
0.4483	-48560.

LA VS DMSO
CM= 0.04614

LIG CON	CAL/MOLE
0.0107	-1354.
0.0213	-2846.
0.0320	-4271.
0.0426	-5705.
0.0533	-7078.
0.0639	-8453.
0.0746	-9789.
0.0852	-11056.
0.0959	-12360.
0.1066	-13630.
0.1172	-14867.
0.1279	-16154.
0.1385	-17408.
0.1492	-18615.
0.1598	-19808.
0.1705	-21018.
0.1811	-22270.
0.1918	-23517.
0.2024	-24758.
0.2131	-25951.
0.2238	-27139.
0.2344	-28385.
0.2451	-29631.
0.2557	-30907.
0.2664	-32107.
0.2770	-33330.
0.2919	-35081.
0.3069	-36778.
0.3197	-38192.
0.3410	-40391.
0.3623	-42352.
0.3857	-44093.
0.4049	-45147.
0.4262	-46119.
0.4475	-46814.
0.4688	-47323.
0.4901	-47682.
0.5114	-47955.
0.5328	-48164.

LA VS DMSO
CM= 0.04614

LIG CON	CAL/MOLE
0.0107	-1557.
0.0213	-3121.
0.0320	-4663.
0.0427	-6177.
0.0534	-7635.
0.0640	-9078.
0.0747	-10479.
0.0854	-11852.
0.0961	-13196.
0.1067	-14498.
0.1174	-15743.
0.1281	-17059.
0.1388	-18368.
0.1494	-19634.
0.1601	-20936.
0.1708	-22132.
0.1815	-23427.
0.1921	-24644.
0.2028	-25896.
0.2135	-27149.
0.2242	-28408.
0.2348	-29682.
0.2562	-32166.
0.2775	-34708.
0.2989	-37227.
0.3202	-39499.
0.3416	-41721.
0.3629	-43709.
0.3843	-45356.
0.4056	-46783.
0.4270	-47755.
0.4483	-48501.
0.4697	-49061.
0.4910	-49508.
0.5123	-49862.
0.5337	-50139.
0.5550	-50351.
0.5764	-50506.
0.5977	-50641.
0.6191	-50754.
0.6404	-50859.
0.6618	-50951.
0.6831	-51021.

NC VS DMSO
CM= 0.01599

LIG CON	CAL/MOLE
0.0064	-460.
0.0128	-2442.
0.0213	-5033.
0.0320	-8196.
0.0427	-11288.
0.0534	-14582.
0.0640	-17981.
0.0747	-21544.
0.0854	-24958.
0.0961	-28361.
0.1067	-31516.
0.1174	-34284.
0.1281	-36564.
0.1494	-39618.
0.1708	-41211.
0.1921	-42091.
0.2135	-42693.
0.2348	-42994.
0.2562	-43297.
0.2775	-43458.

ND VS DMSO
CM= 0.01599

LIG CON	CAL/MOLE
0.0107	-2759.
0.0213	-5851.
0.0320	-8914.
0.0426	-12076.
0.0533	-15410.
0.0639	-18751.
0.0746	-22211.
0.0852	-25551.
0.1066	-31745.
0.1279	-36224.
0.1492	-38895.
0.1705	-40304.
0.1918	-41060.
0.2131	-41516.
0.2344	-41803.
0.2557	-41958.

ND VS DMSO
CM= 0.06142

LIG CON	CAL/MOLE
0.0213	-1671.
0.0427	-3316.
0.0640	-4935.
0.0854	-6518.
0.1067	-8128.
0.1281	-9711.
0.1494	-11355.
0.1708	-13060.
0.1921	-14828.
0.2135	-16587.
0.2348	-18427.
0.2562	-20240.
0.2775	-22089.
0.2989	-23884.
0.3202	-25770.
0.3416	-27582.
0.3629	-29366.
0.3843	-31102.
0.4056	-32828.
0.4270	-34467.
0.4483	-36001.
0.4697	-37361.
0.4910	-38488.
0.5123	-39398.
0.5337	-39965.
0.5550	-40524.
0.5764	-40921.
0.5977	-41220.
0.6191	-41453.
0.6404	-41646.

ND VS DMSO
CM= 0.03035

LIG CON	CAL/MOLE
0.0107	-1510.
0.0213	-3327.
0.0320	-5121.
0.0426	-6813.
0.0533	-8551.
0.0639	-10256.
0.0746	-12038.
0.0852	-13797.
0.0959	-15651.
0.1066	-17364.
0.1172	-19143.
0.1279	-20998.
0.1492	-24772.
0.1705	-28406.
0.1918	-31861.
0.2131	-34984.
0.2344	-37458.
0.2557	-39270.
0.2770	-40403.

ND VS DMSO
CM= 0.06142

LIG CON	CAL/MOLE
0.0213	-1755.
0.0426	-3634.
0.0639	-5489.
0.0852	-7337.
0.1066	-9181.
0.1279	-11059.
0.1492	-12922.
0.1705	-14861.
0.1918	-16805.
0.2131	-18774.
0.2344	-20779.
0.2557	-22809.
0.2770	-24865.
0.2984	-26885.
0.3197	-28910.
0.3410	-30898.
0.3623	-32891.
0.3836	-34837.
0.4049	-36746.
0.4262	-38565.
0.4475	-40273.
0.4688	-41795.
0.4901	-43078.
0.5115	-44100.
0.5328	-44837.
0.5541	-45438.
0.5754	-45848.
0.5967	-46173.
0.6180	-46435.
0.6393	-46644.

ND VS DMSO
CM= 0.04530

LIG CON	CAL/MOLE
0.0064	-577.
0.0128	-1308.
0.0213	-2278.
0.0426	-4544.
0.0639	-6813.
0.0852	-8916.
0.1066	-11160.
0.1279	-13407.
0.1492	-15754.
0.1705	-18061.
0.1918	-20384.
0.2131	-22751.
0.2344	-25050.
0.2557	-27295.
0.2770	-29443.
0.2984	-31537.
0.3197	-33477.
0.3410	-35207.
0.3623	-36642.
0.3836	-37767.
0.4049	-38652.
0.4262	-39325.
0.4475	-39799.
0.4688	-40147.
0.4901	-40424.

ND VS DMSO
CM= 0.04530

LIG CON	CAL/MOLE
0.0213	-2522.
0.0427	-4987.
0.0640	-7435.
0.0854	-9866.
0.1067	-12187.
0.1281	-14649.
0.1494	-17175.
0.1708	-19804.
0.1921	-22415.
0.2135	-25036.
0.2348	-27694.
0.2562	-30293.
0.2775	-32916.
0.2989	-35383.
0.3202	-37707.
0.3416	-39666.
0.3629	-41285.
0.3843	-42547.
0.4056	-43449.
0.4270	-44074.
0.4483	-44489.
0.4697	-44807.
0.4910	-45027.

GD VS DMSO
CM= 0.05991

LIG CON	CAL/MOLE
0.0213	-1436.
0.0427	-2996.
0.0640	-4801.
0.0854	-6672.
0.1067	-8699.
0.1281	-10740.
0.1494	-12919.
0.1708	-15112.
0.1921	-17310.
0.2135	-19502.
0.2348	-21678.
0.2562	-23787.
0.2775	-25900.
0.2989	-28018.
0.3202	-30046.
0.3416	-32121.
0.3629	-34137.
0.3843	-36137.
0.4056	-38057.
0.4270	-39939.
0.4483	-41709.
0.4697	-43293.
0.4910	-44628.
0.5123	-45754.
0.5337	-46606.
0.5550	-47280.
0.5764	-47796.
0.5977	-48195.
0.6191	-48521.
0.6404	-48729.
0.6618	-48938.

GD VS DMSO
CM= 0.01550

LIG CON	CAL/MOLE
0.0107	-2765.
0.0213	-6074.
0.0320	-9678.
0.0426	-13410.
0.0533	-17165.
0.0639	-20922.
0.0746	-24493.
0.0852	-27961.
0.0959	-31222.
0.1066	-34211.
0.1172	-36825.
0.1279	-39020.
0.1492	-41879.
0.1705	-43499.
0.1918	-44445.
0.2131	-45034.
0.2344	-45497.
0.2557	-45812.

GD VS DMSO
CM= 0.05991

LIG CON	CAL/MOLE
0.0213	-1417.
0.0426	-3092.
0.0639	-4909.
0.0852	-6774.
0.1066	-8792.
0.1279	-10849.
0.1492	-13039.
0.1705	-15192.
0.1918	-17394.
0.2131	-19569.
0.2344	-21772.
0.2557	-23938.
0.2770	-26141.
0.2984	-28264.
0.3197	-30413.
0.3410	-32503.
0.3623	-34411.
0.3836	-36456.
0.4049	-38429.
0.4262	-40319.
0.4475	-42102.
0.4688	-43701.
0.4901	-45180.
0.5115	-46373.
0.5328	-47253.
0.5541	-47967.
0.5754	-48446.
0.5967	-48847.
0.6180	-49203.
0.6393	-49480.

GD VS DMSO
CM= 0.01550

LIG CON	CAL/MOLE
0.0107	-2717.
0.0213	-5884.
0.0320	-9363.
0.0427	-13074.
0.0534	-16701.
0.0640	-20266.
0.0747	-23748.
0.0854	-27011.
0.0961	-30113.
0.1067	-32938.
0.1174	-35564.
0.1281	-37544.
0.1494	-40328.
0.1708	-41902.
0.1921	-42776.
0.2135	-43319.
0.2348	-43746.
0.2562	-44038.

HO VS DMSO
CM= 0.05592

LIG CON	CAL/MOLE
0.0213	-1837.
0.0427	-4098.
0.0640	-6472.
0.0854	-8903.
0.1067	-11337.
0.1281	-13717.
0.1494	-16099.
0.1708	-18449.
0.1921	-20712.
0.2135	-22876.
0.2348	-25031.
0.2562	-27188.
0.2775	-29402.
0.2989	-31551.
0.3202	-33735.
0.3416	-35933.
0.3629	-38155.
0.3843	-40356.
0.4056	-42412.
0.4269	-44267.
0.4483	-45729.
0.4696	-46853.
0.4910	-47695.
0.5123	-48380.
0.5337	-48952.
0.5550	-49444.
0.5764	-49858.
0.5977	-50216.
0.6191	-50551.
0.6404	-50829.
0.6618	-51085.

HO VS DMSO
CM= 0.01352

LIG CON	CAL/MOLE
0.0130	-5099.
0.0213	-8628.
0.0320	-13050.
0.0427	-17202.
0.0534	-21021.
0.0640	-24638.
0.0854	-31554.
0.1067	-37382.
0.1281	-40072.
0.1494	-41483.
0.1708	-42452.
0.1921	-43223.
0.2135	-43795.
0.2348	-44257.

HO VS DMSO
CM= 0.05592

LIG CON	CAL/MOLE
0.0213	-2040.
0.0426	-4258.
0.0639	-6558.
0.0852	-8918.
0.1066	-11240.
0.1279	-13590.
0.1492	-15847.
0.1705	-18065.
0.1918	-20211.
0.2131	-22351.
0.2344	-24397.
0.2557	-26515.
0.2770	-28604.
0.2984	-30698.
0.3197	-32841.
0.3410	-34957.
0.3623	-37088.
0.3836	-39123.
0.4049	-41118.
0.4262	-42891.
0.4475	-44316.
0.4733	-45612.
0.4901	-46264.
0.5115	-46967.
0.5328	-47534.
0.5541	-48033.
0.5754	-48419.
0.5967	-48770.
0.6180	-49088.
0.6393	-49360.
0.6606	-49598.

HO VS DMSO
CM= 0.01352

LIG CON	CAL/MOLE
0.0107	-3810.
0.0213	-8227.
0.0320	-12666.
0.0426	-16953.
0.0533	-20806.
0.0639	-24550.
0.0852	-31646.
0.1066	-37614.
0.1279	-40523.
0.1492	-41957.
0.1705	-42871.
0.1918	-43546.
0.2131	-44025.

LU VS DMSO
CM= 0.01484

LIG CON	CAL/MOLE
0.0086	-3324.
0.0172	-6868.
0.0258	-10064.
0.0344	-13245.
0.0430	-15828.
0.0538	-18940.
0.0645	-22055.
0.0753	-25426.
0.0860	-29030.
0.0981	-33217.
0.1075	-35907.
0.1290	-38584.
0.1720	-39587.
0.2151	-40012.

LU VS DMSO
CM= 0.01484

LIG CON	CAL/MOLE
0.0102	-3614.
0.0204	-7627.
0.0307	-11141.
0.0409	-14313.
0.0511	-17285.
0.0613	-20228.
0.0818	-26244.
0.1022	-31895.
0.1227	-36300.
0.1431	-37595.
0.1636	-38090.
0.2045	-38632.

LU VS DMSO
CM= 0.02254

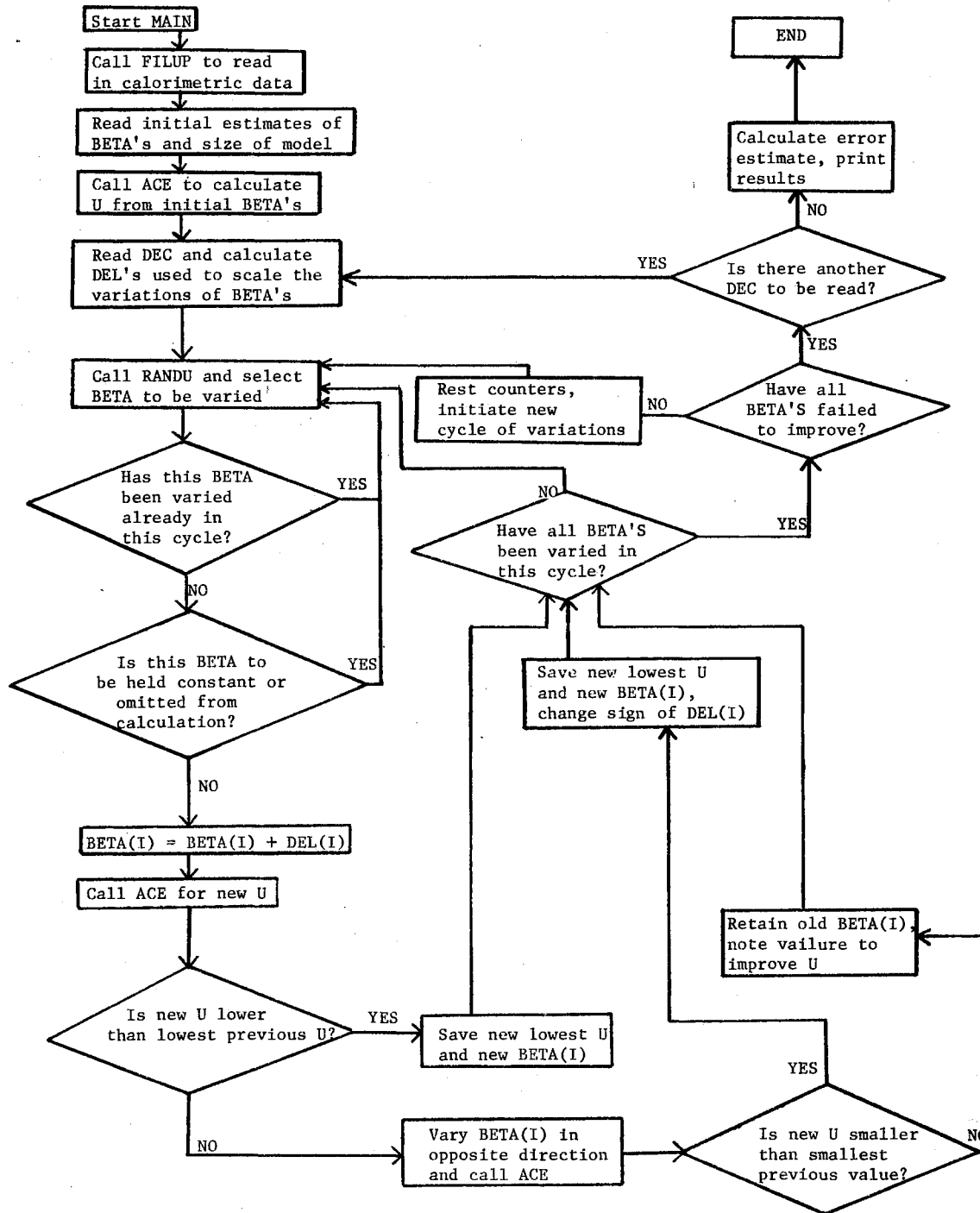
LIG CON	CAL/MOLE
0.0120	-2424.
0.0240	-5820.
0.0400	-10051.
0.0600	-14601.
0.0800	-18799.
0.1000	-22107.
0.1200 ⁺	-26512.
0.1400	-31268.
0.1601	-35922.
0.1801	-39002.
0.2001	-40117.
0.2401	-40858.
0.2801	-41206.

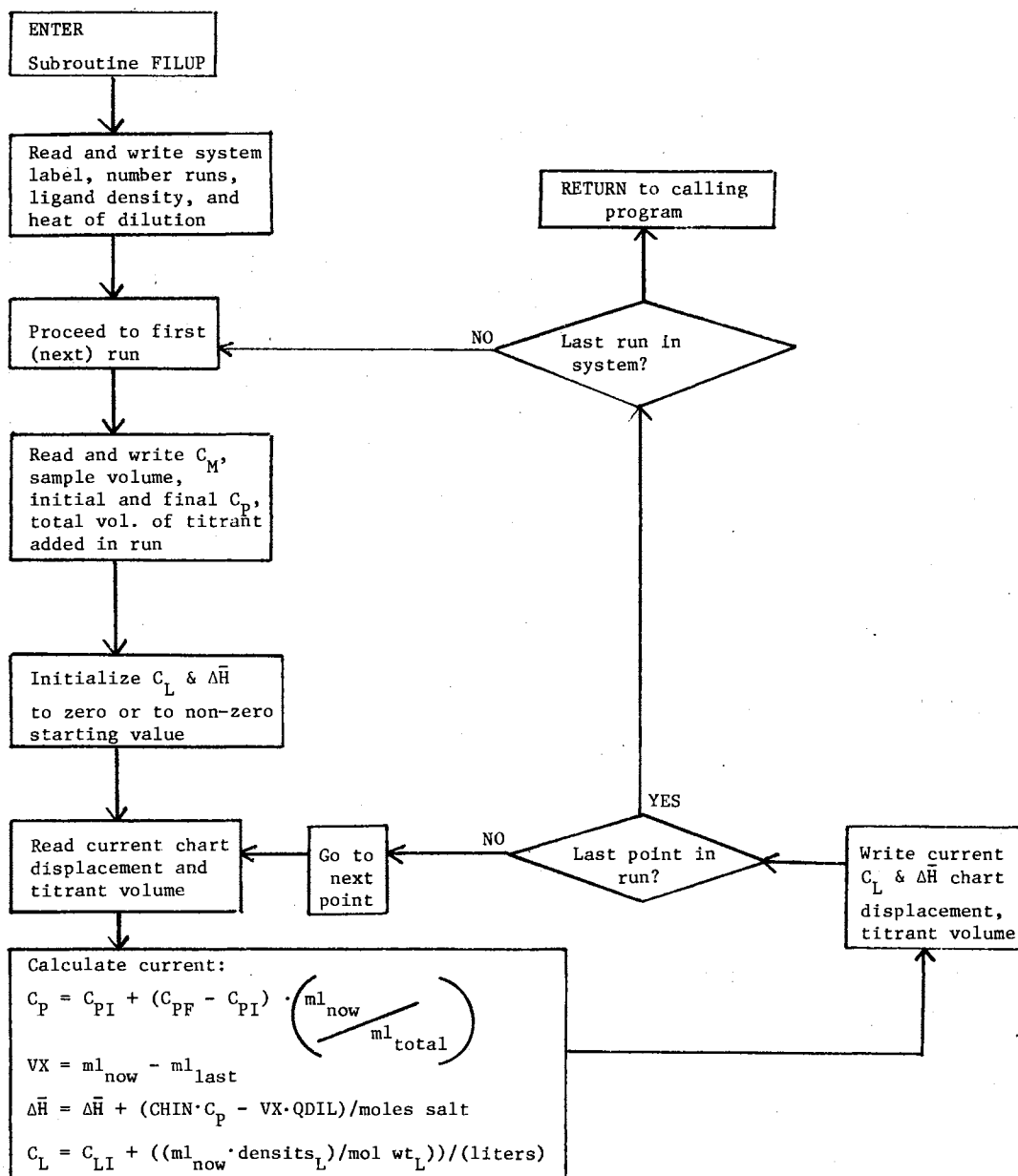
LU VS DMSO
CM= 0.02254

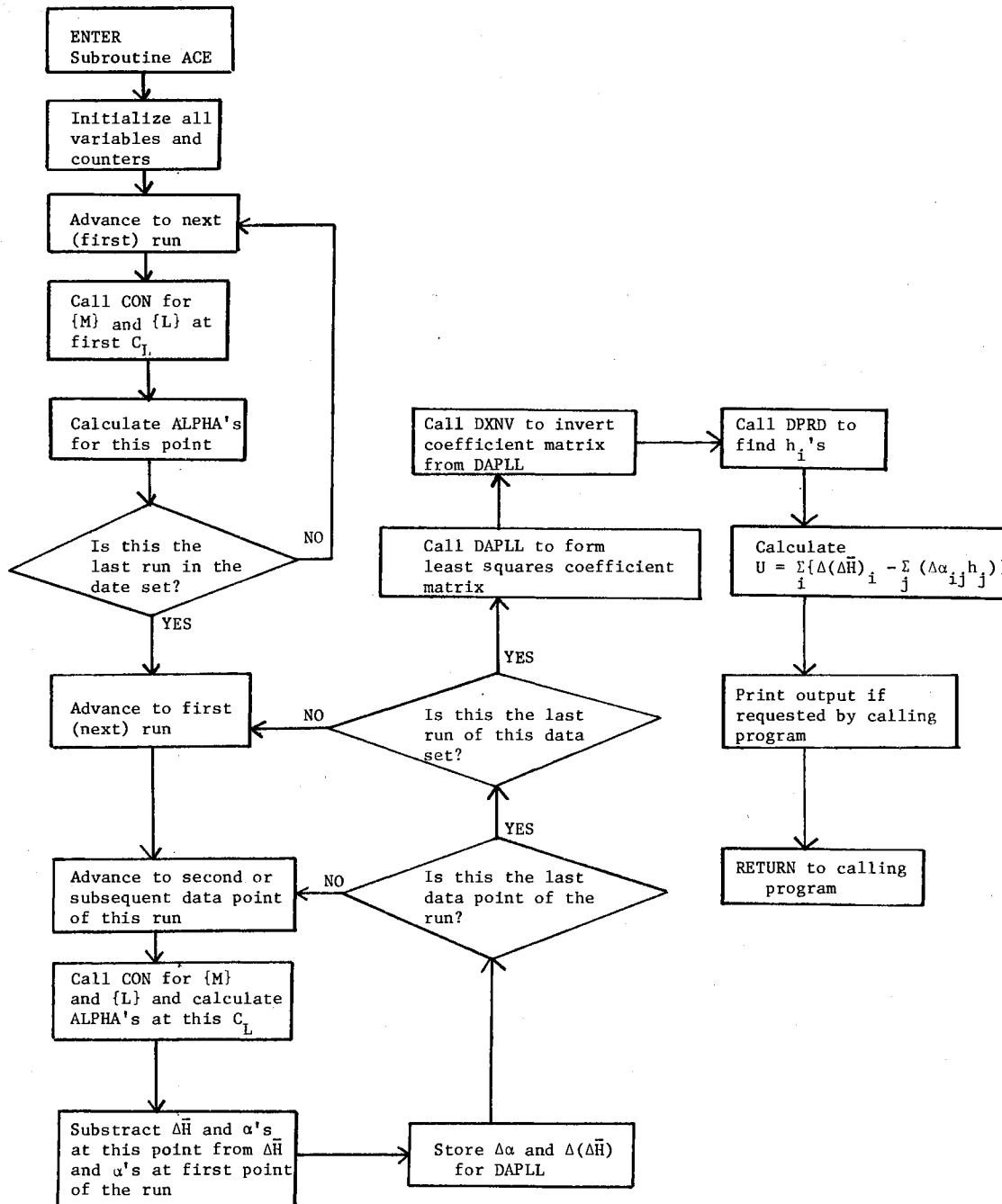
LIG CON	CAL/MOLE
0.0169	-4755.
0.0296	-8429.
0.0423	-11567.
0.0635	-16245.
0.0847	-20791.
0.1059	-25452.
0.1270	-30540.
0.1482	-35900.
0.1694	-40027.
0.1905	-41573.
0.2117	-42154.

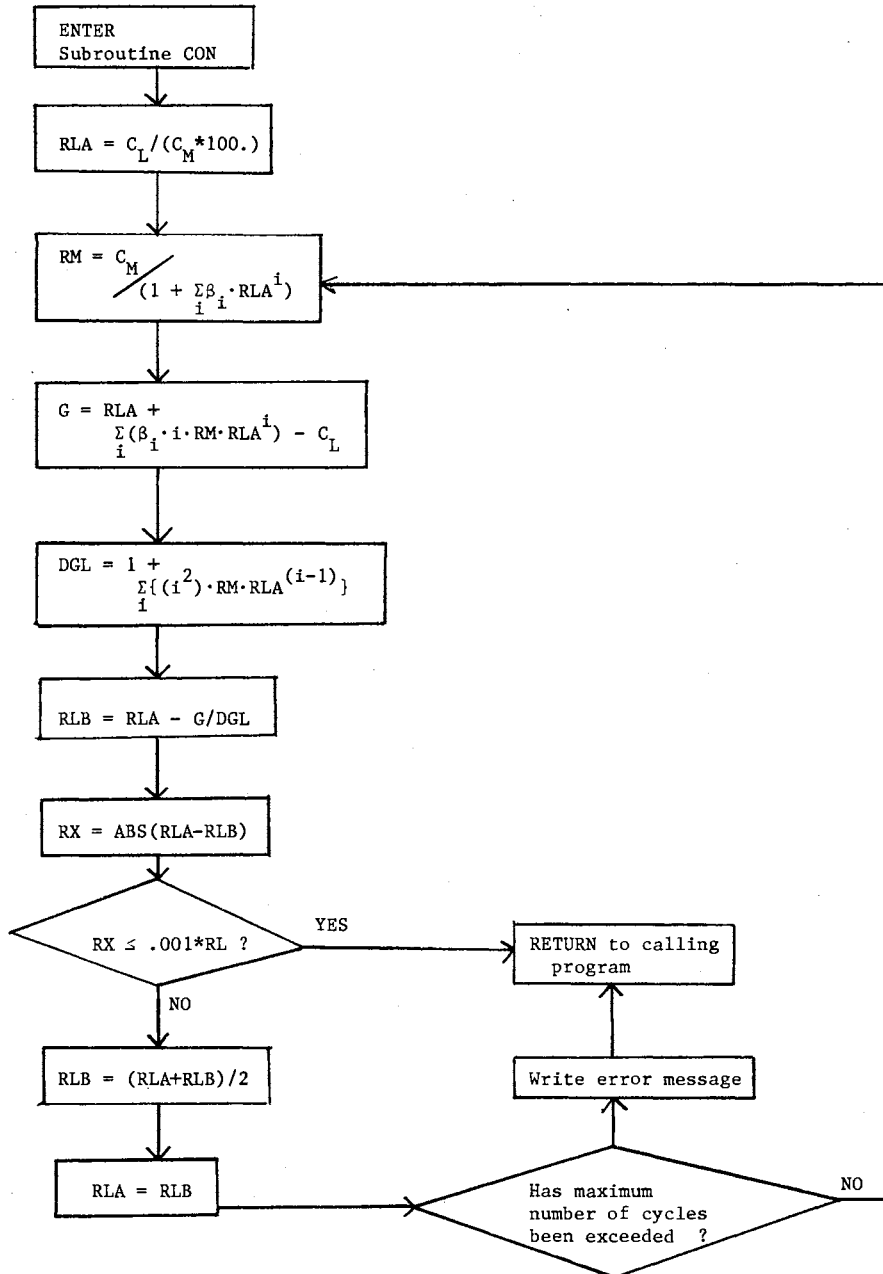
APPENDIX B

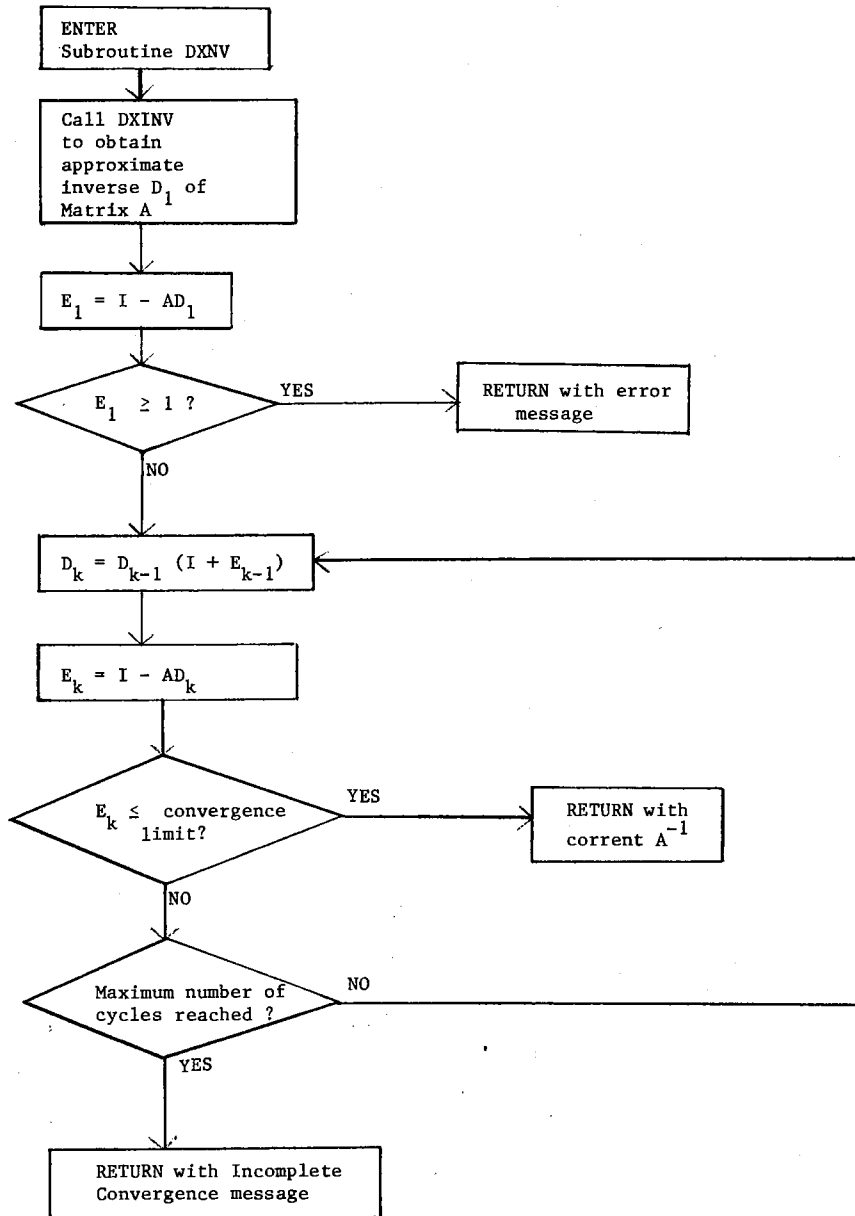
FLOW CHARTS











VITA

James Calvert Cannon

Candidate for the Degree of

Doctor of Philosophy

Thesis: A CALORIMETRIC STUDY OF THE INTERACTIONS OF LANTHANIDE
PERCHLORATES IN ACETONITRILE WITH WATER AND WITH DIMETHYL
SULFOXIDE

Major Field: Chemistry

Biographical:

Personal Data: Born in Tulsa, Oklahoma, November 14, 1947, the
son of Mr. and Mrs. Calvert L. Cannon.

Education: Graduated from Ada High School, Ada, Oklahoma, in
1965; received Bachelor of Science degree in Chemistry from
Oklahoma State University in 1969; enrolled in doctoral
program at Oklahoma State University, 1969-73; completed
requirements for the Doctor of Philosophy degree at Oklahoma
State University in December, 1973.

Professional Experience: Summer Research Participant, Savannah
River Laboratory, 1968; Graduate Teaching Assistant, Oklahoma
State University, 1969-73; Freshman Chemistry Tutor, Oklahoma
State University, College of Engineering, 1973.